

NPS ARCHIVE
1999.03
TUITE, J.

DUDLEY KNOX LIBRARY
NAVAL POSTGRADUATE SCHOOL
MONTEREY CA 93943-5101

NAVAL POSTGRADUATE SCHOOL MONTEREY, CALIFORNIA



THESIS

ENHANCEMENT OF BOILING
IN HIGHLY WETTING FLUIDS

by

Joseph M. Tuite

March 1999

Thesis Advisor:

M. D. Kelleher

Approved for public release; distribution is unlimited.

REPORT DOCUMENTATION PAGE			Form Approved OMB No. 0704-0188	
Public reporting burden for this collection of information is estimated to average 1 hour per response, including the time for reviewing instruction, searching existing data sources, gathering and maintaining the data needed, and completing and reviewing the collection of information. Send comments regarding this burden estimate or any other aspect of this collection of information, including suggestions for reducing this burden, to Washington Headquarters Services, Directorate for Information Operations and Reports, 1215 Jefferson Davis Highway, Suite 1204, Arlington, VA 22202-4302, and to the Office of Management and Budget, Paperwork Reduction Project (0704-0188) Washington DC 20503.				
1. AGENCY USE ONLY (Leave blank)		2. REPORT DATE March 1999	3. REPORT TYPE AND DATES COVERED Master's Thesis	
4. TITLE AND SUBTITLE: Enhancement of Boiling in Highly Wetting Fluids			5. FUNDING NUMBERS	
6. AUTHOR(S) Tuite, Joseph M.				
7. PERFORMING ORGANIZATION NAME(S) AND ADDRESS(ES) Naval Postgraduate School Monterey CA 93943-5000			8. PERFORMING ORGANIZATION REPORT NUMBER	
9. SPONSORING/MONITORING AGENCY NAME(S) AND ADDRESS(ES)			10. SPONSORING/MONITORING AGENCY REPORT NUMBER	
11. SUPPLEMENTARY NOTES The views expressed here are those of the authors and do not reflect the official policy or position of the Department of Defense or the U.S. Government.				
12a. DISTRIBUTION/AVAILABILITY STATEMENT Approved for public release; distribution is unlimited.			12b. DISTRIBUTION CODE	
13. ABSTRACT (maximum 200 words) The boiling of a highly wetting dielectric fluid, in an oscillating environment, has been investigated. Because of low surface tension, these liquids require very high superheat to initiate nucleate boiling. This high degree of superheat required can be reduced by oscillation of the fluid. This oscillation removes the bubbles, which are forming in the nucleation sites on the wire, which allows new bubbles to form. The amplitude and frequency of the oscillation has been varied in an attempt to find optimum values. All attempted oscillation amplitudes and frequencies reduced the required superheat necessary to initiate nucleate boiling. Some oscillation amplitudes and frequencies were more effective than others. No global optimum amplitude or frequency was specifically located. Several local optimum values were found. Once oscillation amplitude was found to produce equal required superheat values at various frequencies, thus appearing to be independent of frequency.				
14. SUBJECT TERMS Boiling Enhancement Techniques			15. NUMBER OF PAGES 118	
			16. PRICE CODE	
17. SECURITY CLASSIFICATION OF REPORT Unclassified	18. SECURITY CLASSIFICATION OF THIS PAGE Unclassified	19. SECURITY CLASSIFICATION OF ABSTRACT Unclassified	20. LIMITATION OF ABSTRACT UL	

Approved for public release; distribution is unlimited.

**ENHANCEMENT OF BOILING
IN HIGHLY WETTING FLUIDS**

Joseph M. Tuite
Lieutenant, United States Navy
B.S. Marine Engineering, U.S. Naval Academy, 1992

Submitted in partial fulfillment of the
requirements for the degree of

MASTER OF SCIENCE IN MECHANICAL ENGINEERING

from the

**NAVAL POSTGRADUATE SCHOOL
March 1999**

ABSTRACT

The boiling of a highly wetting dielectric fluid, in an oscillating fluid environment, has been investigated. Because of low surface tension, these liquids require very high superheat to initiate nucleate boiling. This high degree of superheat required can be reduced by oscillation of the fluid. This oscillation removes the bubbles, which are forming in the nucleation sites on the wire, which allows new bubbles to form. The amplitude and frequency of the oscillation has been varied in an attempt to find the optimum values.

All attempted oscillation amplitudes and frequencies reduced the required superheat necessary to initiate nucleate boiling. Some oscillation amplitudes and frequencies were more effective than others. No global optimum amplitude or frequency was specifically located. Several local optimum values were found. One oscillation amplitude was found to produce equal required superheat values at various frequencies, thus appearing to be independent of frequency

TABLE OF CONTENTS

I.	INTRODUCTION.....	1
A.	BACKGROUND.....	1
B.	PREVIOUS WORK.....	4
C.	OBJECTIVES.....	6
II.	EXPERIMENTAL APPARATUS.....	9
A.	DESCRIPTION OF COMPONENTS.....	9
1.	Main Chamber.....	9
a.	<i>Heaters</i>	11
b.	<i>The Board and Adjustable Spring Assembly</i>	11
c.	<i>Condenser/Heat Exchanger</i>	12
2.	Front Chamber.....	12
3.	DC Motor and Piston/Cylinder Assembly.....	13
B.	INSTRUMENTATION.....	14
1.	Platinum Wire.....	14
2.	Power Supplies.....	15
3.	Data Acquisition System.....	15
4.	Frequency Measurements.....	16
III.	EXPERIMENTAL PROCEDURE.....	25
A.	SYSTEM PREPARATIONS.....	25
B.	DEGASSING.....	25

C.	EXPERIMENTAL PROCEDURE.....	26
D.	DATA ACQUISITION PROGRAM.....	27
E.	DATA REDUCTION.....	28
IV.	RESULTS AND DISCUSSION.....	31
A.	BOILING CURVES OF FC-72.....	31
B.	OSCILLATION EFFECTS ON BOILING CURVE.....	32
1.	Amplitude and Frequency Effects on the Boiling Curve.....	33
a.	<i>Amplitude of 0.117 mm</i>	33
b.	<i>Amplitude of 0.105 mm</i>	33
c.	<i>Amplitude of 0.125 mm</i>	34
C.	AMPLITUDES INDEPENDENT OF FREQUENCY.....	35
D.	FURTHER DISCUSSIONS.....	35
V.	CONCLUSIONS AND RECOMMENDATIONS.....	45
A.	CONCLUSIONS.....	45
B.	RECOMMENDATIONS.....	46
APPENDIX A.	CALIBRATION OF PLATINUM WIRE.....	47
A.	SEM ANALYSIS OF PLATINUM WIRE.....	47
B.	CALIBRATION PROCEDURE IN THE CALIBRATION BATH.....	49

C.	CALIBRATION PROCEDURE IN THE MAIN CHAMBER.....	50
D.	RESULTS AND ERROR ANALYSIS.....	50
APPENDIX B.	SAMPLE CALCULATIONS.....	59
A.	DETERMINATION OF EXPERIEMTAL VALUES.....	59
1.	Condenser temperature.....	59
2.	Fluid bulk temperature.....	59
3.	Current of platinum wire and precision resistor.....	59
4.	Platinum wire resistance value.....	60
5.	Platinum wire surface temperature.....	60
6.	Heat flux from platinum wire.....	60
7.	Piston displacement.....	61
8.	Amplitude of oscillation in the main chamber.....	61
9.	Frequency calculation.....	61
B.	DETERMINATION OF NUMERICAL VALUES.....	62
1.	Film temperature.....	62
2.	Thermal conductivity.....	62
3.	Liquid density.....	62
4.	Kinematic viscosity.....	62
5.	Specific heat.....	62
6.	Thermal expansion coefficient.....	63
7.	Thermal diffusivity.....	63
8.	Prandtl number.....	63

9.	Rayleigh number.....	63
10.	Nusselt number.....	63
11.	Heat flux.....	64
APPENDIX C.	UNCERTAINTY ANALYSIS.....	65
A.	UNCERTAINTY IN SURFACE AREA.....	65
B.	UNCERTAINTY IN POWER.....	66
C.	UNCERTAINTY IN HEAT FLUX.....	67
D.	UNCERTAINTY IN TEMPERATURE.....	67
E.	UNCERTAINTY IN WIRE SURFACE TEMPERATURE.....	68
F.	UNCERTAINTY IN OSCILLATION AMPLITUDE.....	68
G.	UNCERTAINTY IN OSCILLATION FREQUENCY.....	69
APPENDIX D.	COMPUTER PROGRAM.....	71
A.	MAIN DATA ANALYSIS PROGRAM.....	71
APPENDIX E.	EXPERIMENTAL DATA.....	79
A.	HEAT FLUX VS. WALL SUPERHEAT PLOTS.....	79
LIST OF REFERENCES.....		95
INITIAL DISTRIBUTION LIST.....		97

LIST OF TABLES

Table 1.	Comparison of Maximum Wall Superheat Values for Three Non-Oscillating Experiments.....	32
Table 2.	Superheat Values for Oscillating FC-72.....	34
Table 3.	Superheat Values for Oscillating FC-72 at an Amplitude of 0.252 mm.....	35
Table 4.	Calibration Data and Linear Aggression Results.....	52
Table 5.	In-Place Calibration.....	52
Table 6.	Final Calibration Data.....	56
Table 7.	Status of Experimental Runs.....	80

1. Introduction	1
2. Theoretical Framework	10
3. Methodology	25
4. Results	45
5. Discussion	65
6. Conclusion	85
7. References	100
8. Appendix	110
9. Glossary	120
10. Index	130

LIST OF FIGURES

Figure 1.	Overall Schematic of System.....	17
Figure 2.	Main Chamber.....	18
Figure 3.	Board and Adjustable Spring Assembly.....	19
Figure 4.	Condenser/Heat Exchanger.....	20
Figure 5.	Front Chamber.....	21
Figure 6.	DC Motor and Piston/Cylinder Assembly.....	22
Figure 7.	Instrumentation Schematic Diagram.....	23
Figure 8.	Boiling Curve of FC-72.....	38
Figure 9.	Boiling Curve of FC-72 with an Oscillation of Amplitude = 0.117mm And a Frequency = 0.69Hz.....	39
Figure 10.	Boiling Curve of FC-72 with an Oscillation of Amplitude = 0.105mm And a Frequency = 1.4Hz.....	40
Figure 11.	Boiling Curve of FC-72 with an Oscillation of Amplitude = 0.125mm And a Frequency = 1.4Hz.....	41
Figure 12.	Boiling Curve of FC-72 with an Oscillation of Amplitude = 0.252mm And a Frequency = 1.0Hz.....	42
Figure 13.	Results from All Experimental Runs.....	43
Figure 14a.	SEM Pictures of Sample Platinum Wire (666x).....	48
Figure 14b.	SEM Pictures of Sample Platinum Wire (1270x).....	48
Figure 15.	Calibration Curve of Platinum Wire.....	53
Figure 16.	Calibration Curve Fit Compared with Experimental Data.....	54
Figure 17.	In-Place Calibration Data Compared to Calibration Curve Fit.....	55
Figure 18.	Final Calibration Curve of Platinum Wire.....	57

Figure 19.	Final Calibration Curve Compared to Calibration Curve of Platinum Wire.....	58
Figure 20.	Boiling Curve of FC-72 with an Oscillation of Amplitude = 0.117mm And a Frequency = 1.0Hz.....	81
Figure 21.	Boiling Curve of FC-72 with an Oscillation of Amplitude = 0.117mm And a Frequency = 1.2Hz.....	82
Figure 22.	Boiling Curve of FC-72 with an Oscillation of Amplitude = 0.105mm And a Frequency = 0.6Hz.....	83
Figure 23.	Boiling Curve of FC-72 with an Oscillation of Amplitude = 0.105mm And a Frequency = 1.0Hz.....	84
Figure 24.	Boiling Curve of FC-72 with an Oscillation of Amplitude = 0.105mm And a Frequency = 1.2Hz.....	85
Figure 25.	Boiling Curve of FC-72 with an Oscillation of Amplitude = 0.125mm And a Frequency = 0.6Hz.....	86
Figure 26.	Boiling Curve of FC-72 with an Oscillation of Amplitude = 0.125mm And a Frequency = 1.0Hz.....	87
Figure 27.	Boiling Curve of FC-72 with an Oscillation of Amplitude = 0.125mm And a Frequency of 1.2Hz.....	88
Figure 28.	Boiling Curve of FC-72 with an Oscillation of Amplitude = 0.117mm And a Frequency = 1.0Hz.....	89
Figure 29.	Boiling Curve of FC-72 with an Oscillation of Amplitude = 0.117mm And a Frequency = 1.2 Hz.....	90
Figure 30.	Boiling Curve of FC-72 with an Oscillation of Amplitude = 0.117mm And a Frequency = 1.4Hz.....	91
Figure 31.	Boiling Curve of FC-72 with an Oscillation of Amplitude = 0.252mm And a Frequency = 0.3Hz.....	92
Figure 32.	Boiling Curve of FC-72 with an Oscillation of Amplitude = 0.252mm And a Frequency = 1.5 Hz.....	93

NOMENCLATURE

<u>Symbol</u>	<u>Units</u>	<u>Description</u>
$A_{\text{Amplitude}}$	mm	Oscillation Amplitude
$A_{\text{Pt. Wire}}$	m^2	Wire Surface Area
a	mm	Main Chamber Inner Length
b	mm	Main Chamber Inner Width
C_p	$\text{J/kg } ^\circ\text{C}$	Specific Heat
D_{piston}	mm	Piston Diameter
$D_{\text{Pt. Wire}}$	mm	Wire Diameter
f	Hz	Oscillation Frequency
$I_{2\Omega}$	Amps	Precision Resistor Current
$I_{\text{Pt. Wire}}$	Amps	Platinum Wire Current
k	$\text{W/m}^\circ\text{C}$	Thermal Conductivity
$L_{\text{Pt. Wire}}$	mm	Wire Length
L_{stroke}	mm	Piston Stroke Length
Q	W	Power
Q''	W/m^2	Heat Flux
$R_{2\Omega}$	Ohms	Precision Resistor
$R_{\text{Pt. Wire}}$	Ohms	Platinum Wire Resistance
T_{bulk}	C	Fluid Bulk Temperature
T_{cond}	C	Condenser Temperature
T_{film}	C	Film Temperature
T_{period}	s	Oscillation Period

T_{surf}	C	Wire Surface Temperature
$V_{2\Omega}$	Volts	Precision Resistor Voltage Drop
$V_{\text{PT.Wire}}$	Volts	Platinum Wire Voltage Drop
α	m^2/s	Thermal Diffusivity
β	$1/^\circ\text{C}$	Thermal Expansion Coefficient
ρ_l	kg/m^3	Liquid Density
ν	m^2/s	Kinematic Viscosity
Δ_{Piston}	$(\text{mm})^3$	Piston Displacement

UNCERTAINTIES:

$\omega_A, \text{Amplitude}$	m	Uncertainty in Oscillation Amplitude
$\omega_A, \text{Pt. Wire}$	m^2	Uncertainty in Wire Surface Area
ω_a	mm	Uncertainty in Main Chamber Length
ω_b	mm	Uncertainty in Main Chamber Width
ω_D, Piston	mm	Uncertainty in Piston Diameter
ω_D	mm	Uncertainty in Wire Diameter
ω_f	Hz	Uncertainty in Oscillation Frequency
ω_L	mm	Uncertainty in Wire Length
ω_L, Piston	mm	Uncertainty in Piston Stroke
ω_Q	W	Uncertainty in Power
ω_Q''	W/m^2	Uncertainty in Heat Flux

$\omega_{R,2\Omega}$	Ohms	Uncertainty in Precision Resistor
ω_{TC}	C	Uncertainty in Thermocouple Temp
$\omega_{T,Period}$	sec	Uncertainty in Oscillation Period
ω_{Tsurf}	C	Uncertainty in Wire Surface Temp
$\omega_{V,2\Omega}$	Volts	Uncertainty in Precision Resistor Voltage Drop
$\omega_{V,Pt.Wire}$	Volts	Uncertainty in Pt.Wire Voltage

DIMENSIONLESS NUMBERS:

Pr	Prandlt number
Ra_D	Rayleigh number
Nu_D	Nusselt number

ACKNOWLEDGEMENTS

The author would like to express his gratitude towards Professor M. D. Kelleher for his highly experienced guidance, advice, and support towards completion of this thesis. He wishes to thank the members of the Mechanical Engineering Support Shop for their efforts, especially to Mr. Tom Christian whose expertise technical support and patience were invaluable. The author also wishes to thank Mr. Stuart Overlin and Mr. Gerhard Schoenthal for their editorial advice and Mr. David Della Fera for insisting he pursue higher education.

THEORY

The first part of the paper is devoted to the study of the properties of the

operator T defined by the formula

$$Tf(x) = \int_{-\infty}^{\infty} K(x, y) f(y) dy$$

where $K(x, y)$ is a kernel satisfying certain conditions.

In the second part we consider the case when the kernel

satisfies the conditions

and

I. INTRODUCTION

A. BACKGROUND

Electronic equipment has made its way into practically every aspect of modern life, from high-powered computers to toys and appliances. The reliability of the electronics of a system is a major factor in the overall reliability of the system. Electronic components become potential sites for excessive heating due to the fact that they depend on passage of electric current to operate. Continued miniaturization of electronic systems has resulted in a dramatic increase in the amount of heat generated per unit volume. As stated by Cengel [Ref. 1], these heat fluxes are comparable in magnitude to those encountered at nuclear reactors and the surface of the sun. These high rates of heat generation can result in high operating temperatures (in excess of 80° C) for electronic equipment, which could jeopardize its safety and reliability. This excessive heat generation must be properly designed for and controlled to ensure the reliability of the electronic equipment.

Natural and forced convection cooling with air has been the mainstay method for providing the necessary cooling of electronic equipment. The relatively lower heat transfer capabilities of these methods has led designers to investigate the use of immersion cooling with liquids. With immersion cooling the heat generating components are totally immersed in a liquid which is the cooling medium. Immersion cooling is better able to withstand the high heat flux and volumetric heat generation, which are characteristic of high performance computers. Immersion cooling provides two solid advantages over natural and forced convection cooling with air: first, liquids as coolants are more effective than gases due to higher heat capacities; secondly, cooling with liquid has the additional possible capability of

two phase boiling heat transfer. Large amounts of heat can be extracted due to the latent heat of boiling.

If the problem of cooling an electrically heated wire immersed in an otherwise quiescent pool of liquid at its saturation temperature is examined, several heat transfer mechanisms are encountered as the wire temperature is increased. When the wire temperature is only slightly higher than the liquid saturation temperature the only heat transfer mechanism is natural convection in which buoyant forces cause the liquid to rise and cool the wire. This is a relatively inefficient cooling method. This process has been extensively studied and a correlation has been established to predict the amount of heat transferred due to natural convection. Kuehn and Goldstein [Ref. 3] established the most recent natural convection heat transfer correlation for small diameter horizontal circular cylinders.

Dhir states [Ref. 2], as wall superheat (difference between heated surface temperature and liquid saturation temperature; $(T_{\text{surf}} - T_{\text{sat}})$) increases, larger vapor bubbles begin to appear on the heated surface. This is referred to as the onset of nucleate boiling. Vapor or gas trapped in imperfections such as cavities and scratches on the heated surface serve as nucleation sites for bubbles. A wedge shaped imperfection on a surface will trap vapor or gas as long as the static contact angle between the solid surface and the liquid-vapor interface is greater than the wedge angle. A bubble will form if the temperature of the liquid at the tip of the cavity is at least equal to the saturation temperature corresponding to the vapor pressure in the bubble. The balance of forces that act on the bubble dictates the diameter to which the bubble will grow before departing. These forces

are associated with the inertia of the liquid and vapor, the liquid drag on the bubble, buoyancy, and the surface tension. When the buoyancy of the bubble exceeds the surface tension of the liquid and liquid drag forces, the bubble is able to depart the heated surface and rise in the fluid. After departure, cooler liquid from the bulk fills the space vacated by the bubble. When the required superheat is once again achieved at the tip of the cavity, a new bubble starts to form at the same nucleation site and the bubble growth and departure sequence repeats. This repeating process is nucleate boiling.

For highly wetting liquids, only sites of very small size will be active in bubble generation. For these liquids, the expected wall superheat at nucleation should be higher than for partially wetting liquids. This excess superheat necessary to establish nucleate boiling creates a hysteresis in the boiling curve since the heated surface temperature drops once nucleate boiling is fully developed. This phenomenon only occurs during the transition from natural convection heat transfer to nucleate boiling heat transfer. During the transition from nucleate boiling to natural convection heat transfer, there is no temperature overshoot and the heated surface temperature steadily decreases with decreasing wall heat flux. The required excess superheat necessary, to commence nucleate boiling is the major problem with using this method for electronic cooling applications.

Immersion cooling research using dielectric liquids such as Fluorinerts (FC series of 3M Corporation) is still ongoing. The dielectric liquids are a synthetically manufactured fluid derived from common organic compounds by replacement of all carbon-bound hydrogen atoms with fluorine atoms. [Ref. 4] The dielectric liquid used in numerous boiling studies is FC-72. FC-72 has excellent electrical insulating and dielectric

characteristics. The dielectric strength for liquid FC-72 is 38kV/0.1 inch and the vapor phase has a similar value. FC-72 is non-corrosive and has a relatively low saturation temperature of 56 °C at atmospheric pressure. [Ref. 4] These properties of FC-72 make it an excellent choice for electronics cooling.

Conducting boiling experiments with FC-72 does have some problems. FC-72 has very low surface tension, which means it is highly wetting, and therefore has the ability to flow into every small crack or crevice in the heated surface. This makes the initial formation of bubbles very difficult and will result in a large wall superheat to initiate nucleate boiling.

The present study is concerned with investigating methods to achieve a reduction in the wall superheat required to initiate nucleate boiling. The wall superheat, also called temperature overshoot ($T_{\text{surf}} - T_{\text{sat}}$), is a major drawback to using immersion cooling with electronic equipment. The electronic equipment can not withstand the high temperatures created prior to nucleate boiling. One method used to enhance the onset of nucleate boiling, which will also reduce the temperature overshoot, is the mechanical removal of the bubbles from the heated surface. Removal of the bubbles prior to their normal departure will create more nuclei sites at a lower wall temperature. This action will facilitate the onset of nucleate boiling and create a lower required temperature overshoot.

B. PREVIOUS WORK

You, Bar-Cohen, and Simon [Ref. 5] conducted experiments with horizontal cylindrical heater surfaces immersed in FC-72 and R-113, saturated at one atmosphere pressure. They observed the effects of fluid and surface properties and materials on boiling

regimes and on the onset of nucleate boiling. They found the incipience wall superheat for FC-72 was about 25 °C lower and nucleate boiling superheat about 6 °C lower than those values for R-113. They have concluded FC-72 is more advantageous for cooling than R-113.

You, Simon, and Bar-Cohen [Ref. 6] studied enhanced surfaces with more available nucleation sites in immersion cooling with boiling. They were attempting to modify the surface of the computer chip to enhance the onset of nucleate boiling. A particular layering technique was found to lower the wall superheat in boiling when compared to the untreated surface. The new particle layering technique could be applied to computer chips without inducing stress or damaging the chip.

You, Ammermam, and Hong [Ref. 7] conducted a series of pool boiling experiments on saturated, gas saturated, and pure sub-cooled FC-72. The dissolved gases significantly enhanced the transition to nucleate boiling in FC-72. For the present study, You's findings demonstrate the need to ensure that FC-72 has been entirely degassed prior to starting the experiment. This is critical since the only nucleate boiling enhancement desired is fluid oscillation, which will remove the bubbles from the platinum wire. Any remaining dissolved gases in the FC-72 will affect the nucleate boiling and skewer the findings of this study.

Marcellus [Ref. 8] conducted a series of experiments with FC-75 to prove that forced flow can increase the critical heat flux value. This can be accomplished by the rapid removal of the vapor bubbles from the heated surface.

Kelleher, et al. [Ref. 9] conducted experiments on a vertical array of five horizontal platinum wires mounted in a pool of FC-72. Excess wall superheat was necessary to initiate nucleate boiling in the FC-72. Their results show that the bubbles from the upstream source reduced the temperature overshoot on the downstream surface. Using the wake flow from one heated surface to assist in removing bubbles from another heated surface proved to be a successful method for lowering the amount of wall superheat necessary to initiate nucleate boiling.

Turk [Ref.10] studied the effects of oscillating the fluid on reducing the excess superheat. Turk conducted a series of experiments using a platinum wire immersed in a main chamber filled with FC-72. A smaller front chamber was rigidly mounted to the main chamber. The front chamber and main chamber were rigidly connected to a piston/cylinder assembly used to oscillate the fluid inside the main chamber. The platinum wire was used as the heated surface. The amplitude and frequency of the oscillation in the main chamber was varied to attempt to locate an optimum value with a small amount of data. A local optimum value was located at amplitude of 0.117mm at a frequency of 0.69Hz.

C. OBJECTIVES

The purpose of the present study is to continue the work begun by Turk to investigate the effects of fluid oscillation on the onset of nucleate boiling. A similar experimental apparatus with an enhanced data acquisition system was used; a main chamber filled with FC-72 housed the platinum wire. A front chamber mounted to the main chamber and serve as the connection with the piston assembly. One major change is that the piston assembly is not rigidly connected to the front or main chamber. This was

changed in an effort to eliminate any vibrations due to the piston assembly being transmitted to the main chamber and effecting the results. An attempt will be made to find the frequency and amplitude of oscillation that will have the greatest reduction in the excess superheat. Keeping wall superheat as low as possible will reduce the surface heat flux and increase the reliability of the electronic equipment.

The first of these is the fact that the
economy is in a state of recession and
that the government is facing a large
budget deficit. The second is the fact
that the government is facing a large
budget deficit. The third is the fact
that the government is facing a large
budget deficit.

The fourth is the fact that the
government is facing a large budget
deficit. The fifth is the fact that the
government is facing a large budget
deficit. The sixth is the fact that the
government is facing a large budget
deficit. The seventh is the fact that
the government is facing a large budget
deficit. The eighth is the fact that
the government is facing a large budget
deficit.

The ninth is the fact that the
government is facing a large budget
deficit. The tenth is the fact that
the government is facing a large budget
deficit. The eleventh is the fact that
the government is facing a large budget
deficit. The twelfth is the fact that
the government is facing a large budget
deficit. The thirteenth is the fact that
the government is facing a large budget
deficit.

II. EXPERIMENTAL APPARATUS

A. DESCRIPTION OF COMPONENTS

The experimental apparatus (Figure 1) consists of four main parts: the main chamber in which the boiling takes place, the front chamber, the adjustable stroke piston with DC motor which oscillates the fluid, and the condenser system located on the top of the main chamber. The main chamber houses the platinum wire and numerous thermocouples. The front chamber is rigidly mounted to the main chamber and serves as a connection between the tubing leading to the piston/cylinder oscillation generator and the main chamber. Only flexible tubing connects the front chamber and the adjustable stroke piston. The condenser system, which form the top of the main chamber was constructed for this experiment and is designed to be cooled by a constant temperature water bath.

The front and main chambers hold the dielectric fluid FC-72. The front chamber regulates the motion in the fluid, which is caused by the piston and transmits the motion to the main chamber. To prevent lose of FC-72 during degassing, all seams are sealed with Dow Corning 3140 RTV coating and Devcon Corporation Silicone Adhesive to prevent leaks. Also at the clearance between the piston seal on the front chamber, Teflon tape is utilized to prevent leakage.

1. Main Chamber (Figure 2)

The main chamber is a Plexiglas box with an aluminum heat exchanger serving as the top cover. The inner dimensions of the main chamber are 152 x 60 x 152 mm. (Figure 2). An accurate measurement of the main chamber is necessary to calculate the vertical

displacement of the fluid in the main chamber as a function volumetric displacement in the piston/cylinder. This allows a direct correlation of the amplitude of the induced motion of the fluid in the main chamber with the piston stroke length.

A Plexiglas board, which holds the 0.05mm platinum wire, is inserted vertically down the center of the main chamber. The board can be easily placed into or removed from the main chamber by means of two slots on the sidewalls. A tube at the back wall of the main chamber is used to house the necessary wiring for the platinum wire and the numerous thermocouples installed throughout the main chamber. All of the wiring necessary exits via this tube and goes either to the connection board or to the data acquisition system.

The FC-72 needs to be degassed via boiling during the experiment. The FC-72 has is capable of having dissolved air up to 48% by volume in solution. [Ref. 3] Dissolved air in the FC-72 will enhance the heat transfer properties of the fluid and will skew the results. Therefore, bulk heaters have been installed at the bottom of the main chamber. Thermocouples have been installed 2cm above the bottom of the chamber to record the fluid bulk temperature. The main chamber is encased in insulation to reduce the amount of heat loss to the atmosphere. Another important feature of the main chamber is the fluid entrance port. The passage from the front chamber to the main chamber is an oval opening with a porous plug installed to evenly smooth the effects of the pump.

The main chamber consists of three major components: the bulk heaters, the condenser/heat exchanger, and the board with the adjustable spring assembly.

a. Heaters

Three strip heaters have been installed at the bottom of the main chamber. The heaters are used to provide the necessary bulk heating throughout the experiment. The heaters are electric powered and attached to a thin aluminum plate at the bottom of the main chamber. The wiring for the heaters enters the chamber via the tubing at the rear of the unit. During the experiment, the fluid must be maintained close to 56°C, which is saturation temperature for FC-72 at atmospheric pressure.

The dimensions of the each heater, manufactured by MINCO Co., are 125 x 11 mm. The heaters are in parallel connection and all three heaters are used at 2.2 A and 20 V during the degassing process. Two heaters are used during the experiment at 0.6 A and 14 V. For that reason two of the heaters are connected to the power supply with toggle switches. The heaters that remain in operation throughout the experiment are the two located at the rear of the chamber and behind the platinum wire.

b. The Board and Adjustable Spring Assembly (Figure 3)

The 0.05 mm diameter platinum wire and the spring, which is used to provide tension on the wire at all times, are mounted on a removable Plexiglas board that is inserted into the main chamber. The platinum wire has been soldered to the brackets under no tension. The spring assembly can be adjusted to impose the proper amount of tension for the conduct of the experiment. The power supply wires for the platinum wire will enter and exit the main chamber via the exit tubing in the rear of the chamber.

c. Condenser/Heat Exchanger (Figure 4)

An aluminum heat exchanger serves as the cover for the main chamber. This heat exchanger condenses the FC-72 vapor and returns it to the chamber. The heat exchanger is secured to the top of the main chamber by ten screws with a cork gasket inserted between the heat exchanger and the main chamber. The condenser/heat exchanger is 2.5cm thick plate with the bottom 0.6cm solid aluminum. Six grooves, 1.8cm deep, were carved into the plate to serve as passages for the cooling liquid to flow. A Plexiglas cover is mounted on the top of the heat exchanger with a cork gasket inserted between the cover and the heat exchanger. The Plexiglas cover contains the cooling liquid's enter and exit fitting. A pump, which is part of the constant temperature bath, circulates the cooling liquid, which is distilled water. The constant temperature bath, (RTE-111 Refrigerated Bath/Circulator, Model No. 134103201100) is manufactured by the NESLAB Instruments Inc. It has a temperature range of -25 C to 150 C with a temperature stability of +/- 0.01 C. This unit has a 1.9 gallon reservoir and the cooling liquid is transported in 0.25 inch inner diameter tygon tubing. The bath has a microcomputer temperature control system that will continually adjust the system to maintain pump outlet temperature at the set temperature. Thermocouples are installed at the inlet and outlet fitting to the heat exchanger to monitor cooling water temperature change across the heat exchanger.

2. Front Chamber (Figure 5)

The front chamber has been added to the main chamber to assist in removing any irregularities from the flow prior to entry in the main chamber. A porous plug is installed

over the opening into the main chamber to serve as a flow dampener. These irregularities could affect the oscillation of the fluid inside the main chamber. Any interference with the amplitude of oscillation will alter the results of the study.

3. DC Motor and Piston/Cylinder Assembly (Figure 6)

For the experiment, a piston/cylinder assembly has been fabricated to act as the fluid oscillation generator. The piston has an outer diameter of 9.5mm (0.375 inches) and has been designed to create an oscillatory motion in the fluid to assist in the removal of bubbles from the platinum wire.

The piston/cylinder assembly is not rigidly connected to the main chamber. The fluid oscillation is transported through 2.75 feet of flexible rubber tubing that has been coiled to assist in isolating the main chamber. This has been implemented to attempt to prevent any vibrations from the DC motor affecting the main chamber's fluid motion.

The frequency and the amplitude of the oscillatory motion in the main chamber are determined from the variable stroke and frequency of the piston. A slot on the rotating disk connected to the DC motor achieves the variable piston stroke. By adjusting the placement of the connection point in the slot, the stroke length can be adjusted as required. The stroke length will be measured using a depth micrometer with a reference point established on the piston assembly foundation. By varying the stroke length, the amount of FC-72 moving from the piston/cylinder assembly to the main chamber is varied. The stroke length of the piston/cylinder assembly controls the amplitude of oscillation inside the main chamber. A 27 volt, 1 Amp DC motor, achieves the variable frequency. The rotational speed is measured by a micro switch tachometer.

B. INSTRUMENTATION (Figure 7)

The main goal of this experiment is to observe changes in the boiling curve of FC-72 by obtaining the surface temperature of the platinum wire at various surface heat flux values. For that reason the platinum wire temperature vs. resistance dependence is calibrated. The results of the platinum wire calibration is a linear temperature vs. resistance relationship. The platinum wire is connected in series to a precision resistor of known resistance in series. With this arrangement, measuring the voltage drop across the precision resistor allows the current in the platinum wire to be calculated. Next the voltage drop across the platinum wire is measured and the resistance of the wire is then easily calculated. With the known resistance value, the surface temperature of the platinum wire can be obtained from the calibration. Since the voltage drop and current in the platinum wire are known, their product yields the heat transfer rate and division by the surface area of the platinum wire will yield the surface heat flux. [Ref. 9]

The bulk temperature of the fluid and the condenser temperature are measured by thermocouples inside the main chamber. Some additional instrumentation is required to obtain the frequency of the DC motor and the piston. Figure 6 is the wiring diagram of power supplies and data acquisition system without thermocouples.

1. Platinum Wire

The platinum wire is a product of Goodfellow Advanced Materials Ltd. of Cambridge, England. It has 99.9% purity and a nominal diameter of 0.05mm. The active length of the platinum wire is 102.8mm. Observations under a scanning electron microscope of a piece of wire from the same spool revealed a diameter of 51.1 μ m. When

mounting the wire, very careful handling of the wire is required due to its small diameter, especially when moving the wire into the main chamber and when removing the wire from the calibration bath.

2. Power Supplies

In this set of experiments, three DC power supplies are used; one for the platinum wire, one for the bulk heaters, and one for the piston assembly DC motor. These power supplies are:

HP 6289A DC Power Supply 0-50V, 0-1.8A with HP 59501B Isolated DAC/Power Supply Programmer. (HP 6289A provided voltage to the platinum wire and the voltage value is controlled by the Power Supply Programmer and the computer program.)

HP 6268A DC Power Supply 0-24V, 0-12A (to power the bulk heaters.)

HP 6289A DC Power Supply 0-50V, 0-1.8A (to power the DC motor.)

3. Data Acquisition System

All the temperature and voltage measurements are gathered by HP 3852A Data Acquisition and Control Unit via the Unitek desktop computer with Pentium processor. The HP 3852A Data Acquisition system is able to convert temperature data directly from the thermocouple to degrees Celsius. The cards that are used in the data acquisition system are:

- | | |
|----------------------|--|
| 1. Thermocouple card | 44708A 20 channel T-couple Acquisition |
| 2. Voltage card | 44705A 20 channel Guarded Acquisition |

4. Frequency Measurements

A 5001 Universal Counter-Time will be used to measure the period. The frequency will be obtained from this measurement.

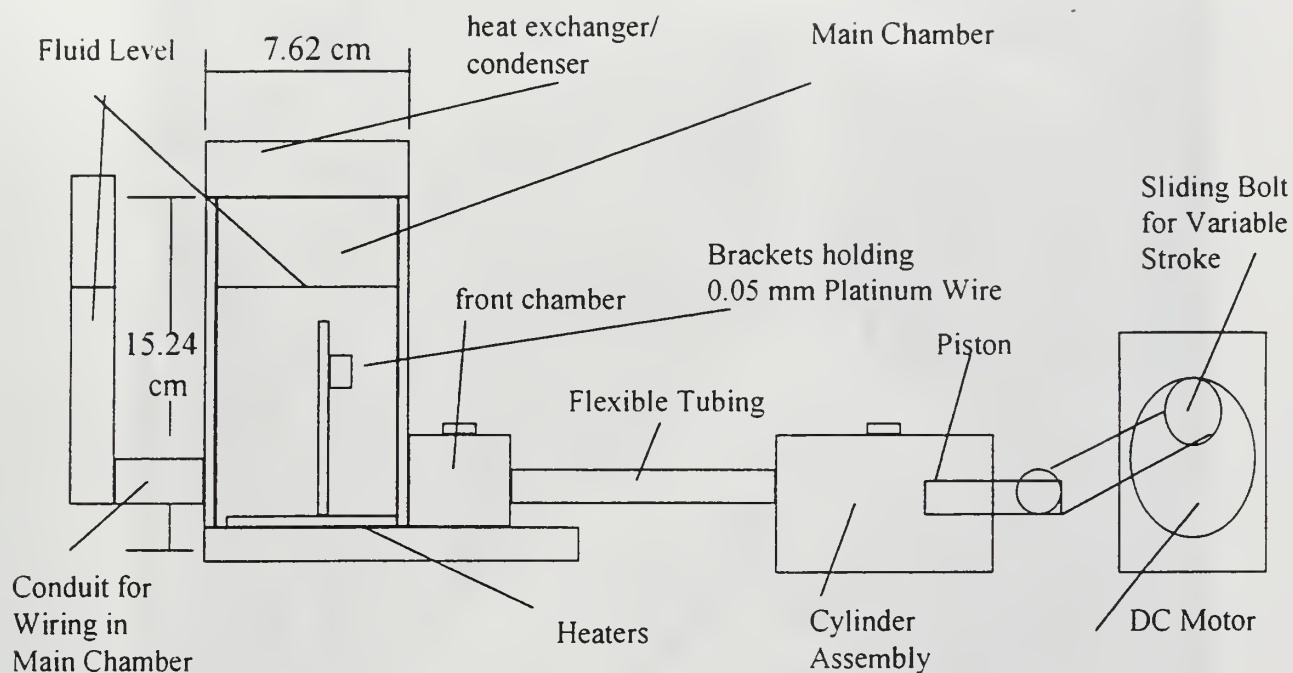


Figure 1. Diagram of Experimental System.

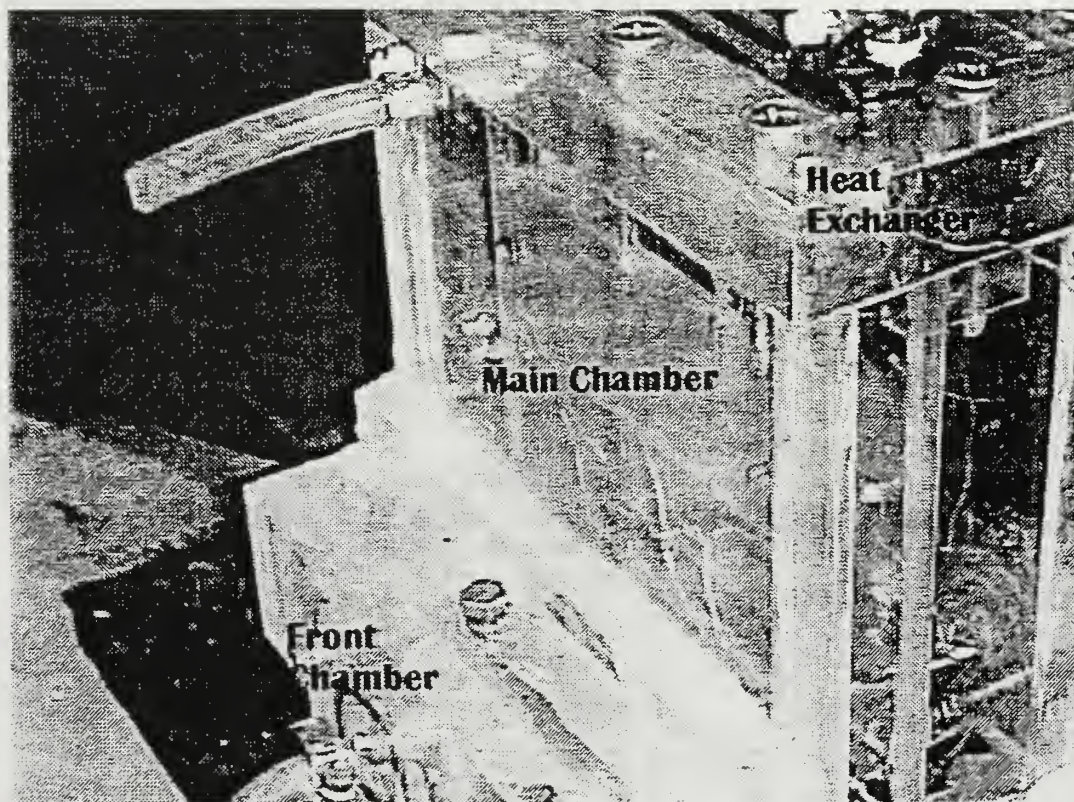


Figure 2. Main Chamber.

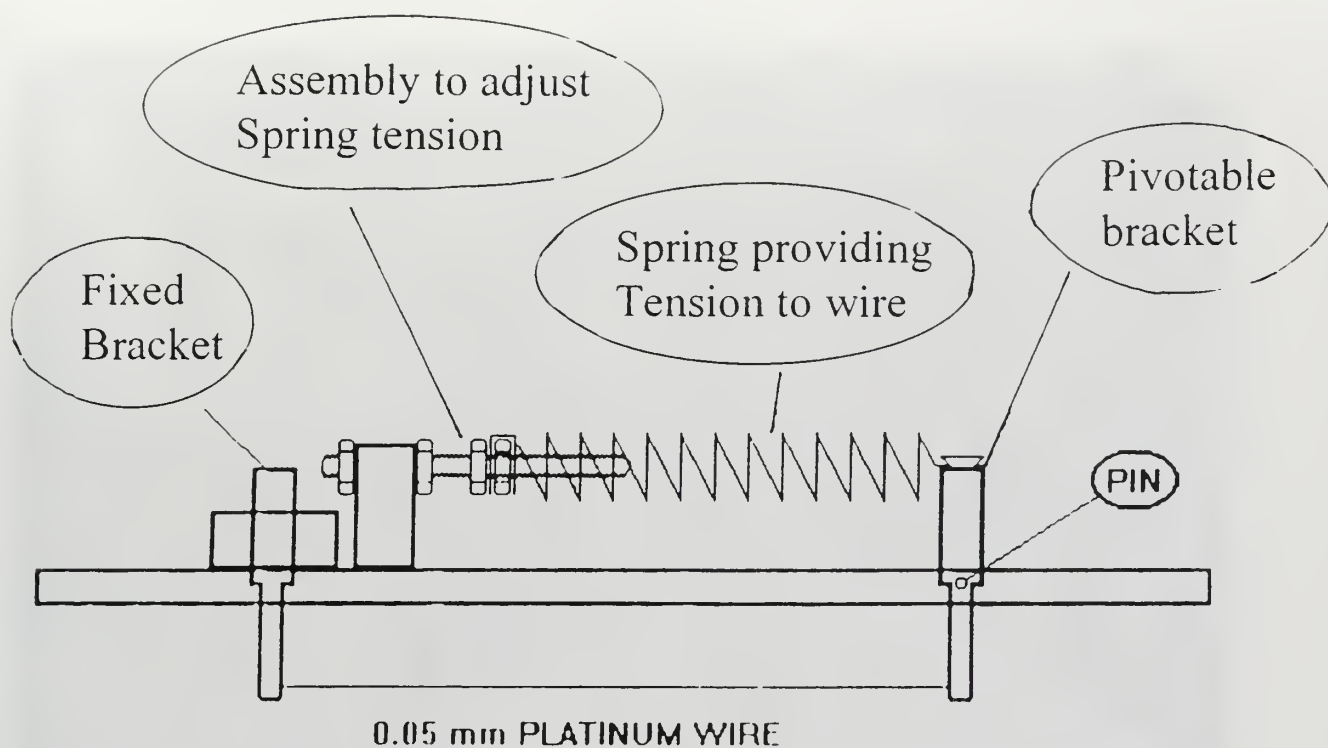


Figure 3. Board and Adjustable Spring Assembly.

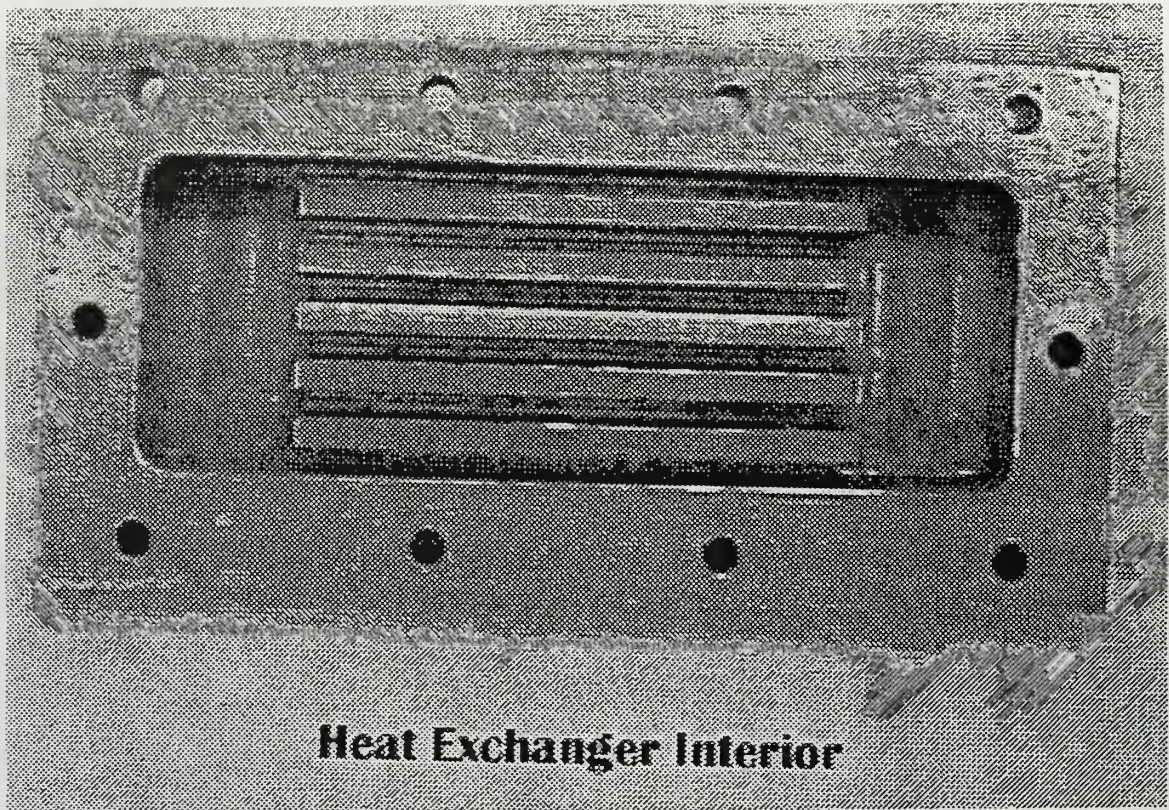


Figure 4. Condenser/Heat Exchanger.

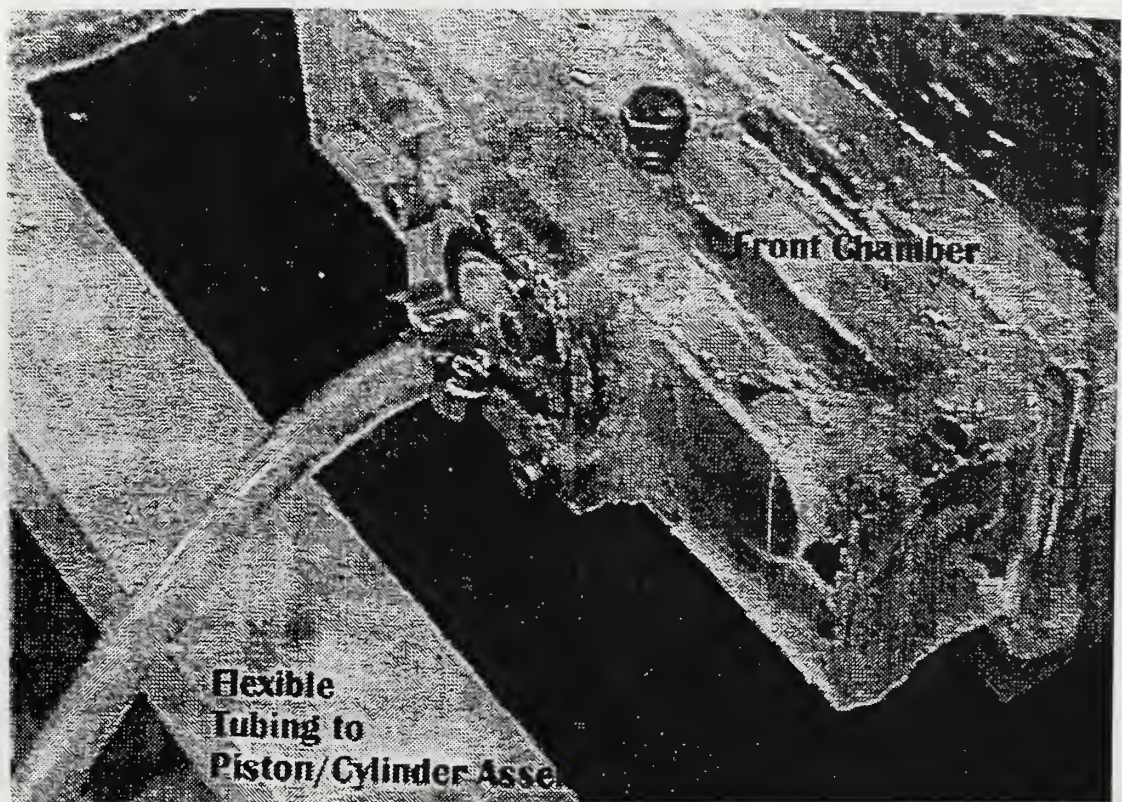


Figure 5. Front Chamber.

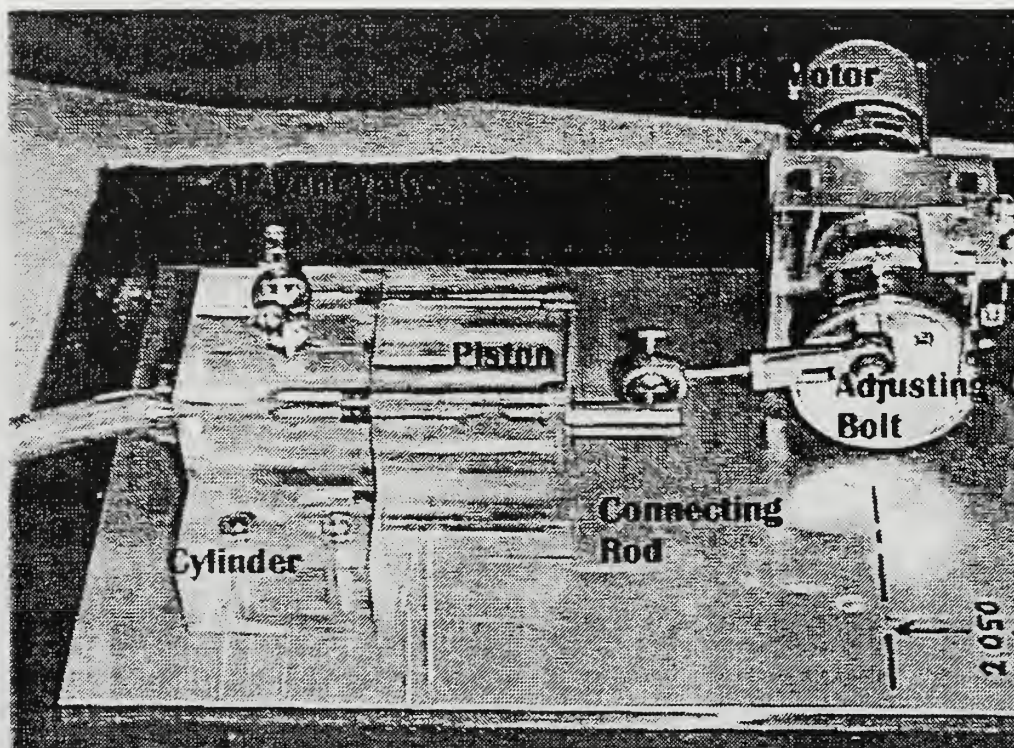


Figure 6. DC Motor and Piston/Cylinder Assembly.

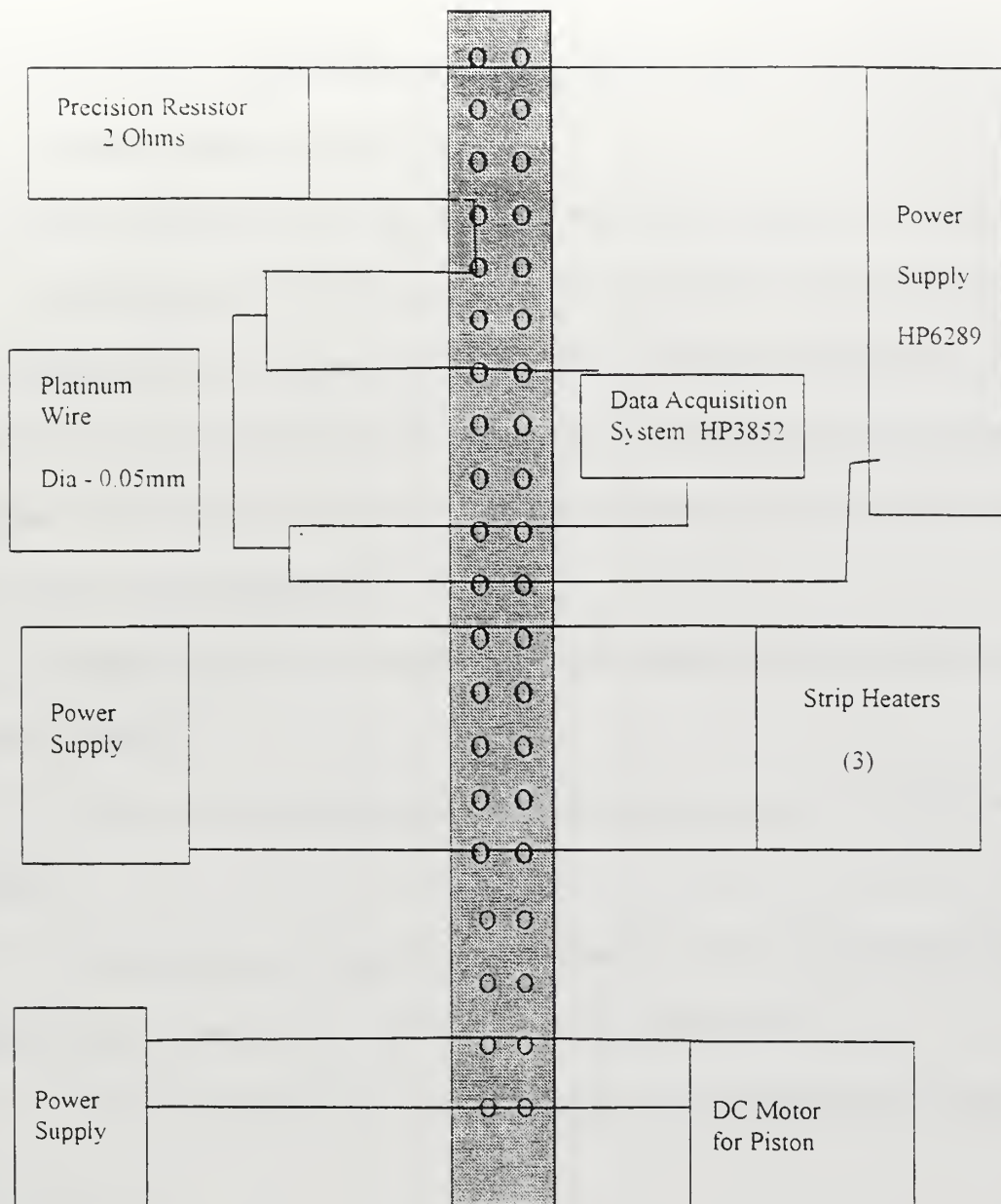


Figure 7. Instrumentation Schematic Diagram.



III. EXPERIMENTAL PROCEDURE

A. SYSTEM PREPARATIONS

Prior to each experimental run, the following preparatory steps must be taken:

1. Check the fluid level of the main chamber and the tube. The fluid level in the main chamber needs to be higher than the platinum wire by, and no higher than, 2.5cm above the top of the platinum wire's Plexiglas mount. The fluid level in the tube should be no higher than the fluid level in the main chamber. If necessary, add more FC-72 via the tube in the rear of the main chamber.
2. Adjust the piston stroke length to the desired setting. Ensure the adjusting bolt is securely fastened.
3. Turn on the HP3852A Data Acquisition System and the Unitek desktop computer.
4. Ensure the heat exchanger is securely fastened to the top of the main chamber and the constant temperature bath reservoir level is at the high mark.
5. The main chamber must be fully insulated during degassing and during the experiment.

B. DEGASSING

Once system preparations are completed, the following steps are to be accomplished to ensure proper degassing of the FC-72:

1. Power all three bulk heaters using the HP 6268A DC Power Supply at 20 V and 2.2 A. Be sure that the top two toggle switches, which are on the connection board, are on.

2. Turn on the constant temperature bath. Set the bath temperature at 20 °C.

Check system fully to ensure that no leaks are present.

Watch the fluid temperature increase and the temperature drop across the heat exchanger steady out at ± 0.3 °C. The fluid temperature should rise up to the saturation temperature of 56 °C. At this temperature degassing will commence with pool boiling. The complete degassing process takes approximately 3 hours to complete.

C. EXPERIMENTAL PROCEDURE

The following steps are to be followed before commencing the experiment:

1. Turn off the bulk heater using the toggle switch at the top of the connection board.
2. Decrease the power of the remaining heaters to 12 V and 0.6 A. Wait until the temperature drops down to a thermal equilibrium point.
3. Turn on the 5001 Universal Counter-Timer.
4. Power DC motor by turning on the HP 6289A DC Power Supply. Adjust the DC motor voltage to obtain the desirable frequency. Verify the desired frequency has been obtained via the Universal Counter-Timer display. Once properly set; use toggle switch on connection board to stop motor.
5. Turn on the HP6289A DC Power Supply and HP59501B Isolated DAC/Power Supply to power the platinum wire and the precision resistor.
6. Load the QBASIC computer program named Tuite1.exe
7. Run first four power setting without running the DC motor for the piston.
8. Save each data set to a 3.5 inch disk inserted in drive A.

9. At the end of the fourth power setting, turn on the DC motor for the piston at the connection board via the toggle switch.

D. DATA ACQUISITION PROGRAM

Data acquisition is accomplished using a QBASIC program called Tuitel.exe.

1. The data acquisition program executes these operations:

Sets up communication with the HP3852A and HP6289A DC Power Supply.

Controls power settings incrementally by the help of HP59501B Power Supply Programmer.

Reads thermocouple temperatures after the HP3852A Data Acquisition System converts the thermocouple voltages to temperature values ($^{\circ}\text{C}$).

Reads voltage drops across the precision resistor and the platinum wire.

Stores all recorded values into a data file either to the hard drive or a 3.5 inch diskette.

2. For each power setting these measurements will be taken once a steady state has been reached.

Bulk temperature (four thermocouples).

Ambient temperature (two thermocouples).

Heat exchanger inlet temperature (one thermocouple).

Heat exchanger outlet temperature (one thermocouple).

Platinum wire voltage drop.

Precision resistor voltage drop.

3. The first five steps of power setting; the voltage increment is 0.5 V. After step five, the increment will be 0.4 V for the next four power settings. After step eight the increment will be 0.2 V until step 22. At the end of the 22nd reading, the power setting will start to decrease by 0.4 V per step. After the end of the 31st reading, the power setting will be decreased by 0.5 V per step and will end after the 35th reading at 1.0 V.

4. Repeat the same steps for all other piston stroke and frequency configurations.

E. DATA REDUCTION

The following calculations are used to reduce the raw data obtained by experiments.

1. Condenser temperature:

$$T_{\text{cond}} (^{\circ}\text{C}) = \frac{(T_0 + T_1 + T_2 + T_3)}{4}$$

T_0 through T_3 are thermocouple temperatures.

2. Fluid bulk temperatures:

$$T_{\text{bulk}} (^{\circ}\text{C}) = \frac{(T_4 + T_5 + T_6 + T_7)}{4}$$

T_4 through T_7 are thermocouple temperatures.

3. Current of platinum wire and precision resistor:

$$I_{\text{Pt. Wire}} (\text{A}) = I_{2\Omega} = \frac{V_{2\Omega}}{R_{2\Omega}}$$

Where $R_{2\Omega} = 2.03\Omega$ (Precision Resistor)

4. Platinum wire resistance value:

$$R_{Pt.Wire}(\Omega) = \frac{V_{Pt.Wire}}{I_{Pt.Wire}}$$

5. Platinum wire surface temperature:

$$T_{surf} (^{\circ}C) = \varepsilon * R_{Pt.Wire} + T_{y=0}$$

where:

$$\varepsilon = 49.689 \quad (\text{slope of calibration curve})$$

$$T_{y=0} = -253.836 \quad (\text{y axis intercept of calibration})$$

6. Fluid film temperature:

$$T_{film}(^{\circ}C) = \frac{T_{surf} + T_{bulk}}{2.0}$$

7. Heat flux from platinum wire:

$$q''(W/m^2) = \frac{I_{Pt.Wire} * V_{Pt.Wire}}{A_{Pt.Wire}}$$

8. Piston displacement:

$$\Delta_{Piston}(mm^3) = \frac{\pi}{4} * D_{Piston}^2 * L_{Stroke}$$

9. Amplitude of oscillation in the main chamber:

$$A_{Amplitude}(mm) = \frac{\Delta_{Piston}}{a * b}$$

Where a and b are the inner length and width of the main chamber.

9. Frequency calculation:

$$f(\text{Hz}) = \frac{1}{T_{\text{Period}}(s)}$$

A MATLAB program was written to evaluate the gathered data. The program was written in three parts. The first part would retrieve the gathered data from the appropriate data file and apply the temperature corrections for the thermocouples. The second part would calculate the heat flux based on the gathered data and the calculated surface temperature of the platinum wire. Next the program would calculate the natural convection using the recommended correlation by Kuehn and Goldstein [Ref. 2] for natural convection around small horizontal cylinders. Then both sets of results are plotted versus the temperature superheat value. For fluid properties, Egger's thesis [Ref. 11] is used.

IV. RESULTS AND DISCUSSION

In the present study, the boiling curve of FC-72 is determined in a non-oscillating bulk fluid. Changes in the boiling curve of FC-72, specifically the value of the wall superheat at the initiation of nucleate boiling, are observed when the bulk fluid is oscillating at different amplitudes and frequencies. All experiments are conducted at atmospheric pressure, 21°C ambient temperature, and the same platinum wire of 0.0511mm diameter is used.

The results of these experiments are presented in the plots of wire heat flux vs. wall superheat ($T_{\text{surf}} - T_{\text{sat}}$). Figures 8 through 12 are a representative sample of the data gathered during the experiments. The remaining graphs are included in APPENDIX E. Figure 8 is the boiling curve of FC-72 without any oscillation in the bulk fluid. The hysteresis between the increasing and the decreasing heat flux shows the amount of wall superheat necessary for the initiation of nucleate boiling. The surface temperature of the wire decreased abruptly with the initiation of nucleate boiling. Figure 10 is the boiling curve of FC-72 with an amplitude of oscillation of 0.105mm and an oscillation frequency of 1.4Hz. The decrease in the magnitude of the hysteresis is obvious when compared to Figure 8.

A. BOILING CURVE OF FC-72 (BOILING WITHOUT OSCILLATION)

To study the effects of oscillation on the boiling curve of FC-72, it is necessary to establish the boiling curve of FC-72 without oscillation of the bulk fluid. The boiling curve of FC-72 under non-oscillating condition will be the base line for comparison for subsequent experiments. Three experiments, Experiments 4, 6, and 25, were conducted

under non-oscillating conditions. The results of Experiment 6 are shown in Figure 8. Experiments 4 and 25 results are in agreement with Experiment 6 and are included in APPENDIX E. The maximum wall superheat ($T_{\text{surf}} - T_{\text{sat}}$) value prior to nucleate boiling was 45°C for this part of the experiment. Maximum wall superheat values for each experiment in this section are listed in Table 1. The fluid bulk temperature was maintained between 51°C and 52.5°C for this experiment. In the natural convection phase of the boiling curve of FC-72, the data is in agreement, within uncertainty limits, with the correlation suggested by Keuhn and Goldstein [Ref. 3] for natural convection heat transfer around small diameter cylinders. The platinum wire surface temperature just after the initiation of nucleate boiling is 19.9% less than the maximum wall superheat value. The percent drop in platinum wire surface temperature just after the initiation of nucleate boiling is in agreement with Egger's results. [Ref. 11].

Experiment Number	Wall superheat necessary to initiate nucleate boiling (°C)
4	45.3
6	45.0
25	45.7

Table 1. The Comparison of Maximum Wall Superheat Values for Three Non-Oscillating Experiments.

B. OSCILLATION EFFECTS ON THE BOILING CURVE

Four different oscillation amplitudes in the fluid surrounding the platinum wire were employed during the study. Turk [Ref. 10] reported a local optimum oscillation amplitude of 0.117mm, which was used in this study as a starting point. Oscillation

amplitudes of 0.105, 0.125, and 0.252mm respectively were also used at various frequencies ranging from 0.3 to 1.5Hz respectively.

1. Amplitude and Frequency Effects on the Boiling Curve

Table 1 represents the maximum wall superheat values observed prior to the initiation of nucleate boiling for the non-oscillating and oscillating FC-72.

a. *Amplitude of 0.117 mm*

The oscillation amplitude of 0.117mm was identified as a local optimum value for oscillation amplitude in Turk's report. [Ref. 10]. The experiment was conducted using oscillation frequencies of 0.69, 1.0, 1.2, and 1.4Hz respectively. The lowest wall superheat value to initiate nucleate boiling was 29.1°C, which is a 33% drop from the boiling curve of FC-72, and was obtained at an oscillation frequency of 0.69Hz. The heat flux vs. wall superheat plot of this frequency is Figure 9. Wall superheat values at various frequencies are listed in Table 2. The best results in the wall superheat drops are achieved at this amplitude. As the frequency of oscillation was increased the wall superheat necessary to initiate nucleate boiling also increased with a maximum value of 37.2°C at 1.4 Hz. Even the maximum value of wall superheat is a 20.9% drop in wall superheat compared to the non-oscillating values. Wire surface temperature and heat flux at various frequencies are listed in Table 2. The remaining heat flux vs. wall superheat plots are included in APPENDIX E.

b. *Amplitude of 0.105 mm*

The oscillation amplitude of 0.105mm, which is approximately two wire diameters in size, produced a decrease in the wall superheat value necessary to initiate

Amplitude	0.105 mm			0.117 mm			0.125 mm		
Frequency (Hz)	Wire Temp (°C)	Bulk Temp (°C)	Heat Flux (W/m ²)	Wire Temp (°C)	Bulk Temp (°C)	Heat Flux (W/m ²)	Wire Temp (°C)	Bulk Temp (°C)	Heat Flux (W/m ²)
No Stroke	101.1	52.9	81,300	101.1	52.9	81,300	101.1	52.9	81,300
0.6	93.3	53.3	84,072	--	--	--	98.5	52.3	90,295
0.69	-	--	--	85.2	52.2	76,082	--	--	--
1.0	90.1	53.1	82,947	86.0	51.3	92,474	91.5	51.8	75,443
1.2	87.9	52.7	68,104	90.0	52.4	75,836	91.7	52.1	75,895
1.4	86.2	52.7	100,000	92.5	53.6	75,313	98.7	53.2	90,309

Table 2. Superheat Values for Oscillating FC-72. For No-Stroke Case the Results of Experiment 6 is Used.

nucleate boiling as the oscillation frequency was increased. The oscillation frequency of 1.4Hz produced a wall superheat value of 30.5°C. The heat flux vs. wall superheat plot for this frequency is Figure 10. This is an improvement from a value of 37.2°C for wall superheat that was achieved at an oscillation frequency of 0.6Hz. Wire surface temperature and heat flux for various frequencies are listed in Table 2. The remaining heat flux vs. wall superheat plots for this amplitude are included in APPENDIX E.

c. Amplitude of 0.125 mm

The oscillation amplitude of 0.125mm, which is approximately 2.5 wire diameters, produced an erratic decrease in wall superheat values necessary to initiate nucleate boiling. A minimum wall superheat value of 35.4°C was achieved at an oscillation frequency of 1.0 and 35.8°C at 1.2Hz respectively. A higher wall superheat value was recorded at oscillation amplitudes of 0.6Hz and 1.4Hz. The heat flux vs. wall superheat plot for a frequency of 1.4 Hz is Figure 11. At an amplitude of 0.125mm, the maximum value of wall superheat is an 8% drop in wall superheat compared to the non-oscillating

value. Wall superheat values at various frequencies are listed in Table 2. The remaining heat flux vs. wall superheat plots for this amplitude are included in APPENDIX E.

C. AMPLITUDES INDEPENDENT OF FREQUENCY

At an amplitude of oscillation of 0.252mm, which is approximately 5 wire diameters, the wall superheat value necessary to initiate nucleate boiling appears to be independent of oscillation frequency. Oscillation frequencies of 0.3, 1.0, and 1.5 Hz respectively were employed and all three produced a wall superheat value of $30.5^{\circ}\text{C} \pm 0.5^{\circ}\text{C}$. The heat flux vs. wall superheat plot for a frequency of 1.0Hz is Figure 12. Wall superheat values at various frequencies are included in Table 3. The remaining heat flux vs. wall superheat plots for this amplitude are included in APPENDIX E.

Amplitude	0.252 mm		
Frequency (Hz)	Wire Temp ($^{\circ}\text{C}$)	Bulk Temp ($^{\circ}\text{C}$)	Heat Flux (W/m^2)
0.3	87.3	51.1	69,542
1.0	86.95	51.5	69,874
1.5	86.6	51.1	83,334

Table 3. Superheat Values for Oscillating FC-72 at an Amplitude of 0.252 mm.

D. FURTHER DISCUSSIONS

A total of 32 experiments have been conducted to achieve the boiling curve of FC-72 at various fluid oscillation amplitudes and frequencies. The effects of the fluid oscillation amplitude and frequencies on the wall superheat, which is necessary to initiate nucleate boiling, have been observed. Figure 13 shows the maximum wall superheat values required to initiate nucleate boiling at four different amplitudes and various frequencies. An overall result of the oscillatory condition is a certain decrease in required

wall superheat for boiling incipience. The oscillation amplitude of 0.117mm at an oscillation frequency of 0.69Hz is the most effective combination attempted during this study.

The reduction of wall superheat necessary to initiate nucleate boiling can be attributed to the way bubbles forming at the nucleation sites depart from the heated surface. When the bubble outgrows the nucleation site, it starts to grow bigger on the wire surface. In highly wetting fluids like FC-72, the bubbles can not depart the surface easily due to low surface tension of the fluid so the surface temperature of the heated surface continues to increase. The bubble departing process from nucleation sites and the heated surface is accelerated due to the oscillation. The oscillations assist the bubbles overcoming the surface tension effects of highly wetting FC-72 by mechanically removing the bubbles. As was expected, some amplitudes and frequencies of oscillation were more effective than others at reducing wall superheat values necessary to initiate nucleate boiling. It is very important to consider that in every case involving fluid oscillation the value of required wall superheat was lower than in the non-oscillating fluid case.

In Figures 8 to 32 These Symbols Are Used:

- X Increasing Heat Flux ($T_{\text{surf}} - T_{\text{sat}}$)
- O Decreasing Heat Flux ($T_{\text{surf}} - T_{\text{sat}}$)
- + Increasing Heat Flux (T_{bulk})
- . Decreasing Heat Flux (T_{bulk})
- Kuehn-Goldstein Correlation (Natural Convection)

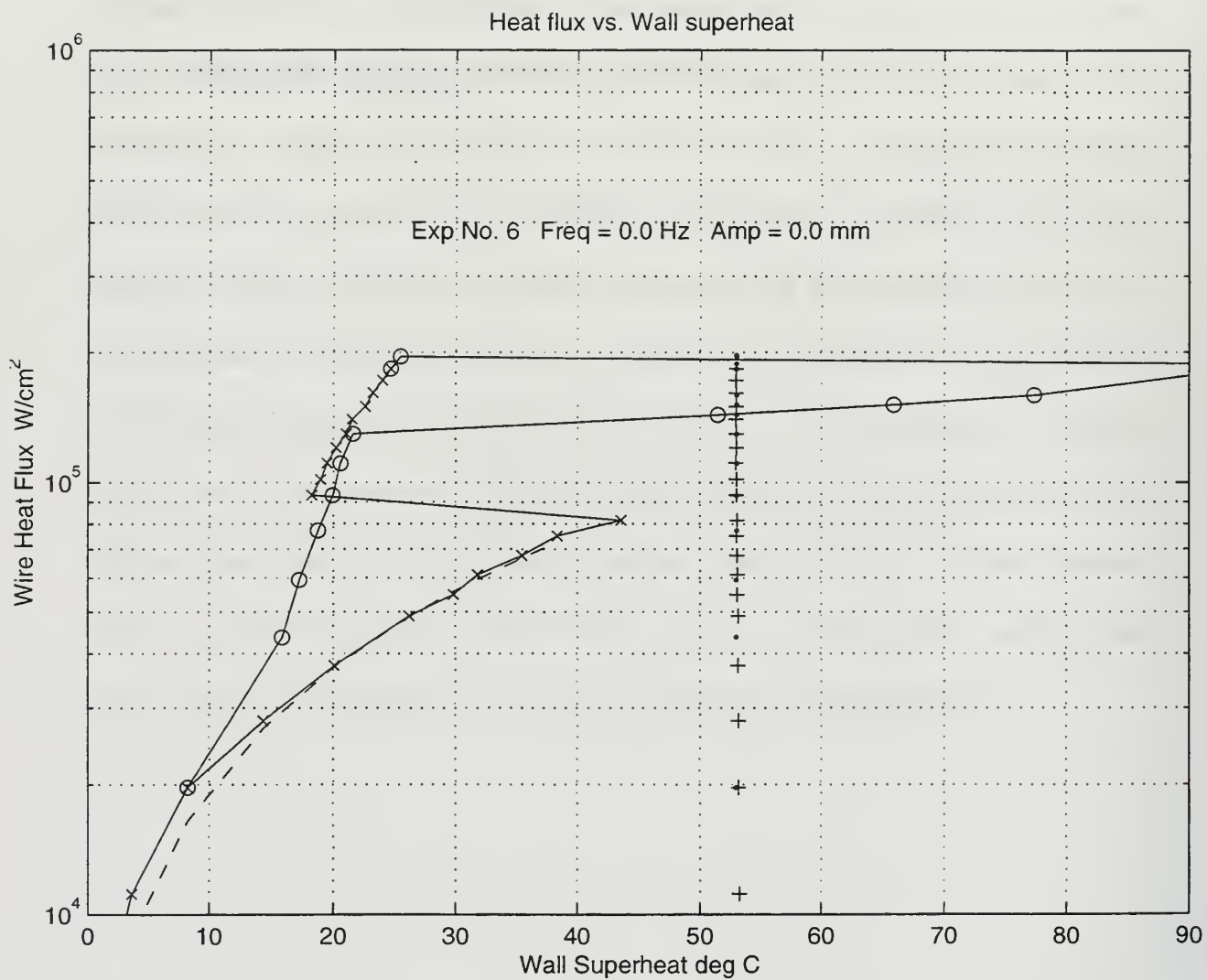


Figure 8. Boiling Curve of FC-72.

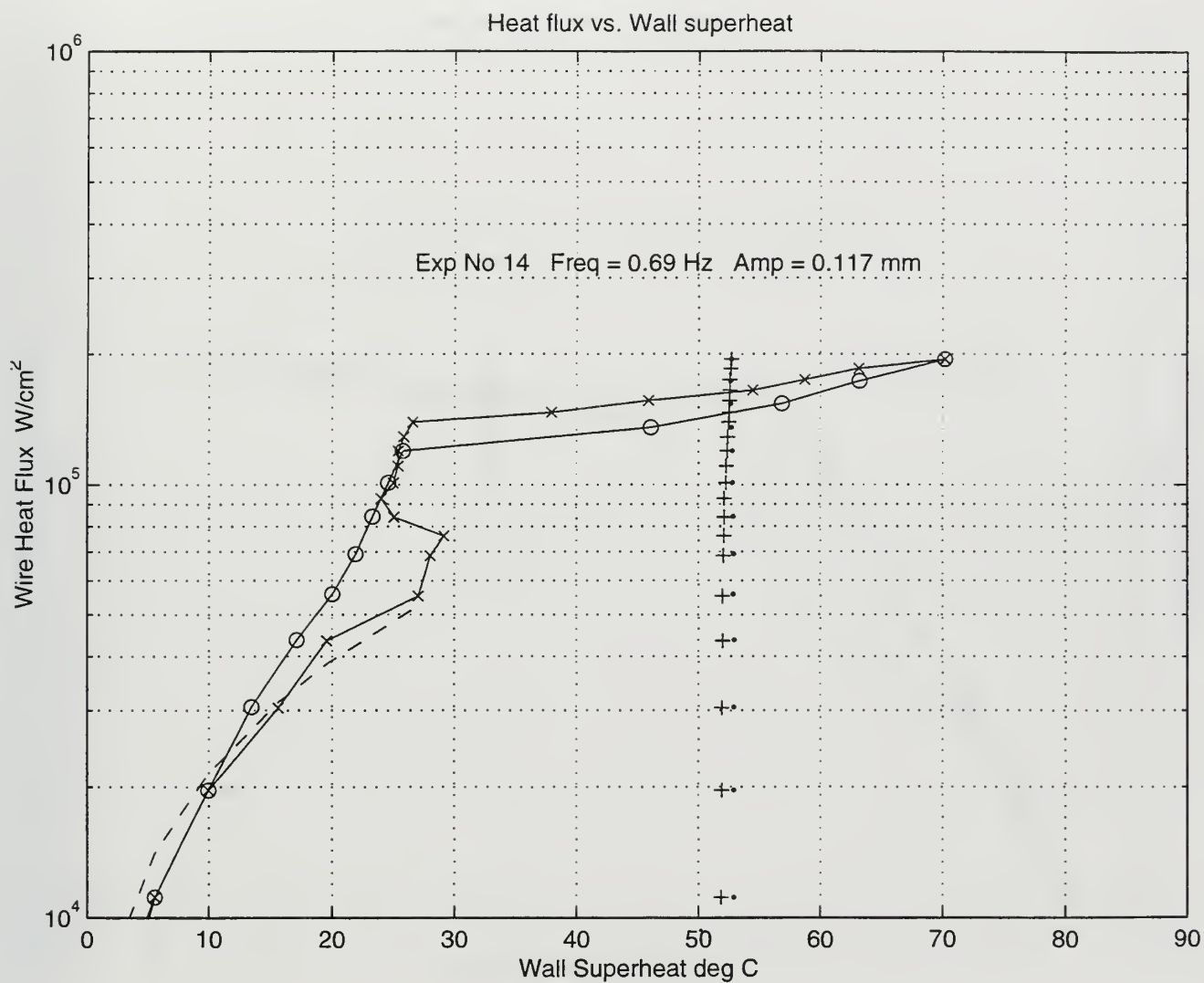


Figure 9. Boiling Curve of FC-72 with an Oscillation of Amplitude 0.117mm And a Frequency of 0.69Hz.

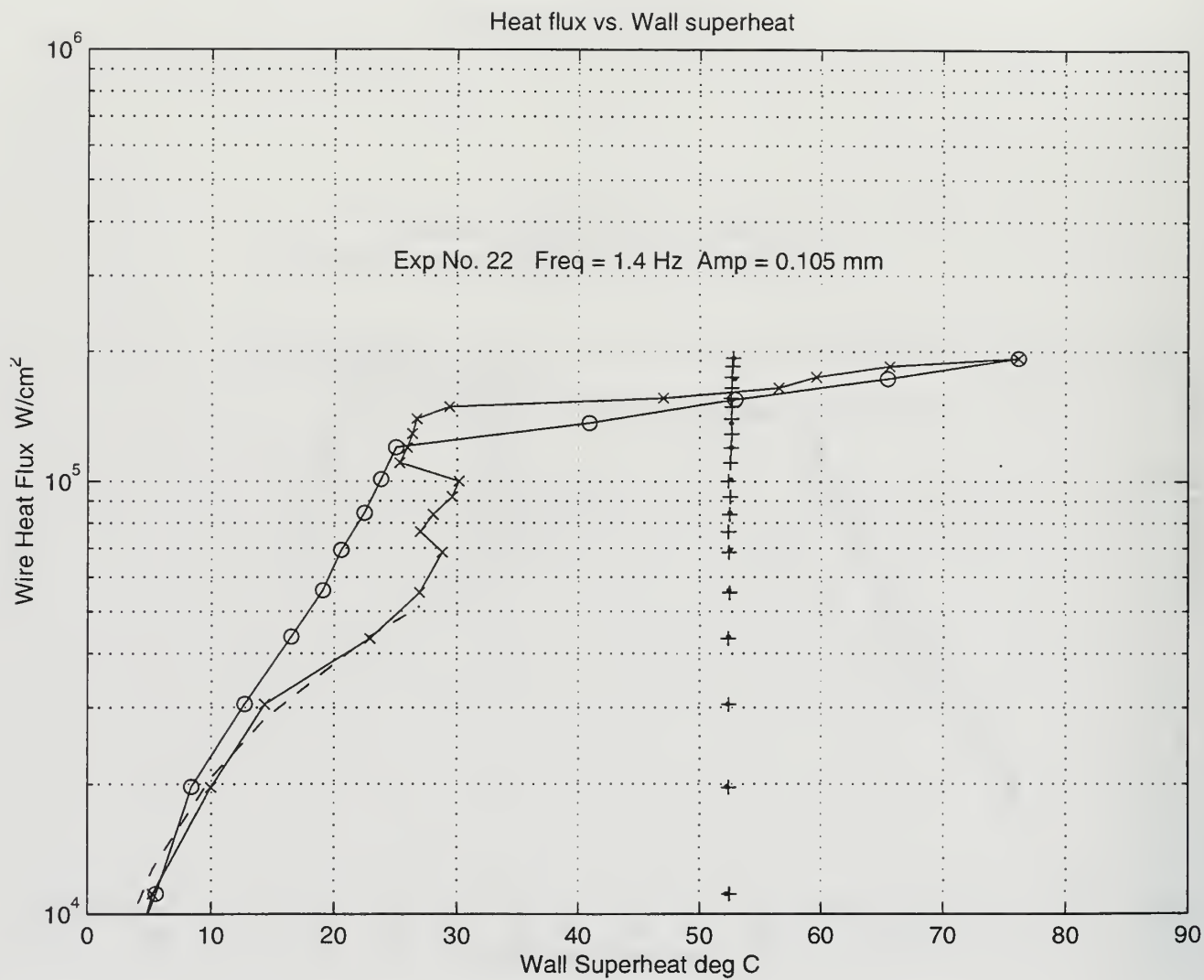


Figure 10. Boiling Curve of FC-72 with an Oscillation of Amplitude 0.105mm And a Frequency of 1.4Hz.

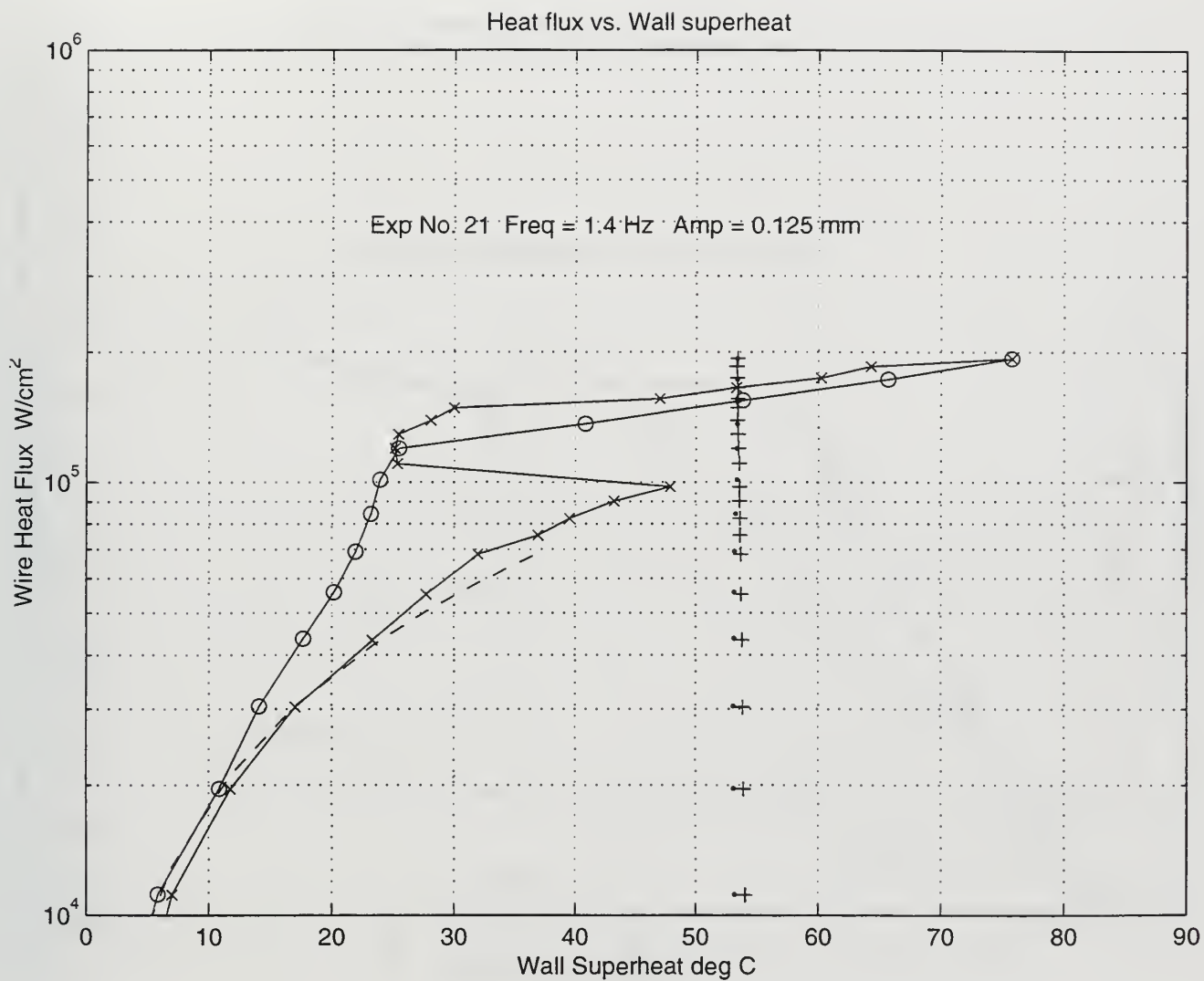


Figure 11. Boiling Curve of FC-72 with an Oscillation of Amplitude 0.125mm And a Frequency of 1.4Hz.

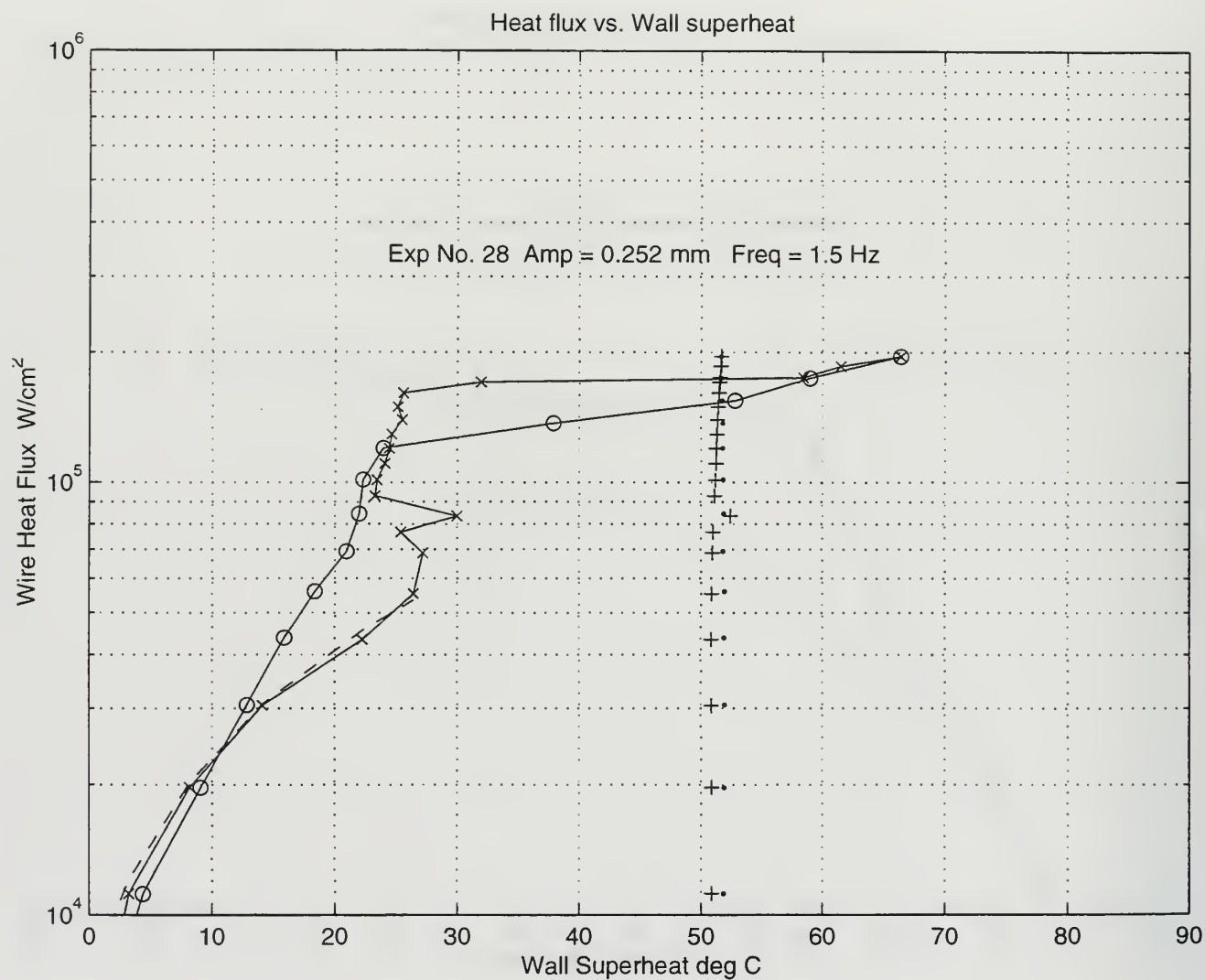


Figure 12. Boiling Curve of FC-72 with an Oscillation of Amplitude 0.252mm And a Frequency of 1.5Hz.

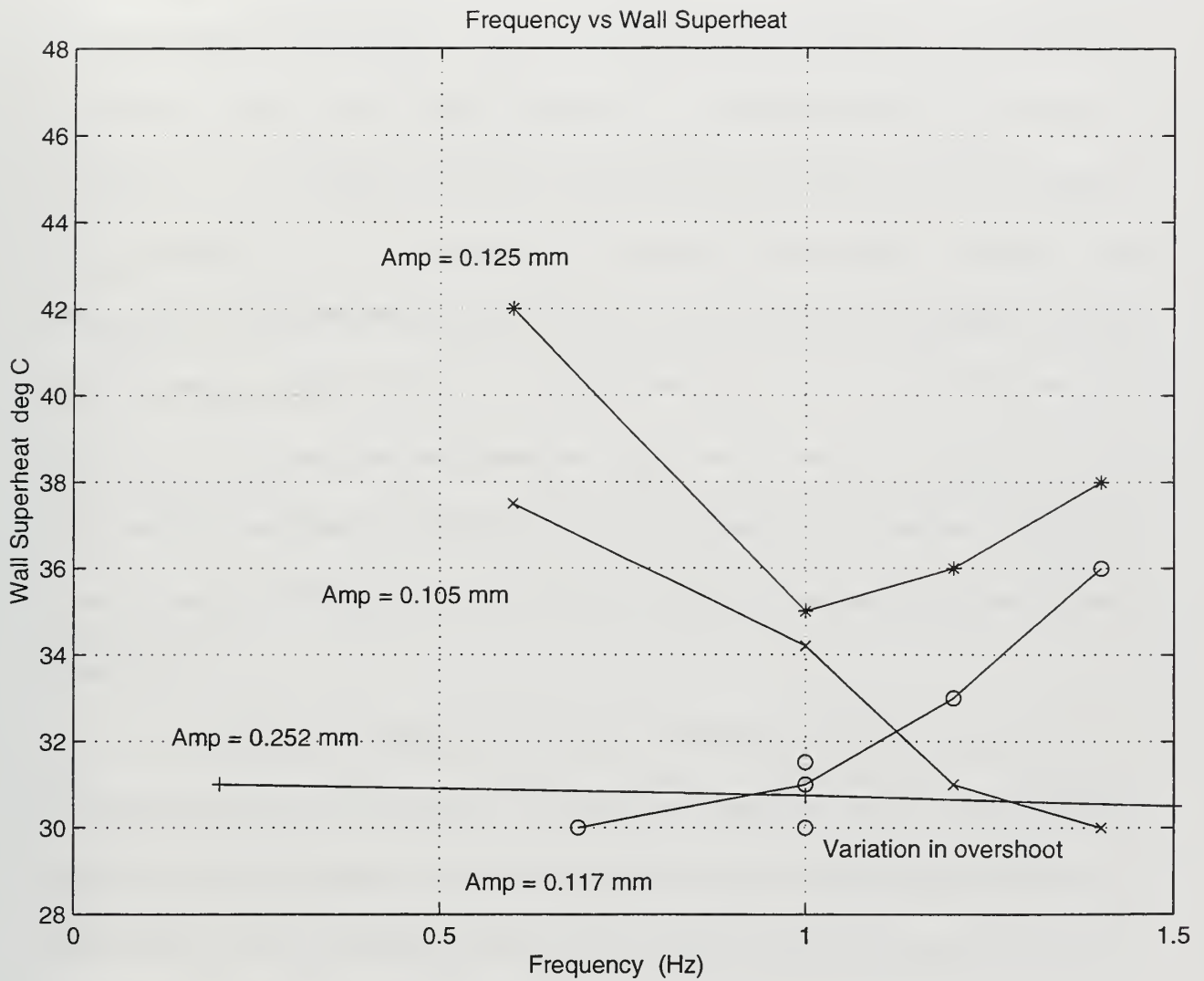


Figure 13. Results of Experiments – Heat Flux vs. Wall Superheat at Various Amplitude and Frequencies of Oscillation.

V. CONCLUSIONS AND RECOMMENDATIONS

A. CONCLUSIONS

The present study investigated boiling of degassed FC-72 in an oscillating fluid condition. An enhancement of the transition to nucleate boiling has been confirmed by the results achieved in this study. All attempted oscillation amplitudes and frequencies changed the boiling curve of highly wetting FC-72. The largest required wall superheat value ($T_{\text{surf}} - T_{\text{sat}}$) necessary to initiate nucleate boiling was recorded in the non-oscillating fluid experiment. At some amplitudes the required wall superheat decreased with increasing oscillation frequency while other cases had the required wall superheat increase with increasing oscillation frequency. The amplitude of 0.117mm and the frequency of 0.69Hz provided the lowest wall superheat temperature for nucleate boiling at 29.1°C. The oscillation amplitude of 0.252mm appeared to be independent of oscillation frequency since a required wall superheat value of 30.5°C \pm 0.5°C was achieved at three different frequencies.

Even though the experiments, which are conducted in this study, proved to be reproducible with uncertainty limits, in the nucleate boiling phase the wall superheat value displayed an erratic behavior. This was expected due to the unsteady nature of the boiling phenomena. No two experiments will be able to exactly reproduce the same results due to the haphazard nature of boiling at the bubble level.

Here it is possible to conclude that the required wall superheat value necessary to initiate nucleate boiling can be decreased with oscillation in the bulk fluid. The reason can be attributed to the oscillating fluid removing the bubbles from the heated surface prior to

their normal departure time. This makes nucleation sites available for future bubble growth at a quicker rate than normal. These nucleation sites are now acting in a more efficient manner and are able to activate other sites as well. This will enhance the transition to nucleate boiling and will reduce the required wall superheat value. These results are in agreement with the results in Turk [Ref.10] and Egger [Ref. 11].

B. RECOMMENDATIONS

In this study only four amplitudes of oscillation were tested at selected frequencies. For future study a more detailed frequency and amplitude map should be created. Also, at the oscillation amplitude of 0.252mm, the required wall superheat necessary to initiate nucleate boiling appeared to be independent of frequency. Continue experiments at oscillation amplitudes between the last two amplitudes tested, 0.125 and 0.252mm respectively, to attempt to locate, if one exists, an oscillation amplitude where wall superheat effects are truly independent of frequency.

During the study numerous experimental runs needed to be abandoned due to leaks in the main chamber. The highly wetting FC-72 penetrated all seams in the structure, including seams coated with sealant. A new experimental apparatus needs to be fabricated using a one piece mold for the main chamber. Since the piston/cylinder assembly is no longer rigidly attached to the main chamber, the front chamber can be smaller and be fabricated as part of the main chamber.

APPENDIX A. CALIBRATION OF PLATINUM WIRE

For this study a platinum wire is used as a temperature reading device. The purpose of this calibration exercise is to establish a relationship between the resistance of the platinum wire and its surface temperature. This relationship is known to be linear. The amount of change in the resistance of the platinum wire can be calibrated to measure temperature. Turk [Ref. 10] used this same process.

Nikuyama [Ref. 11] used the platinum wire as a temperature reading device in the experiments to determine the boiling regime of water. He used a platinum wire to identify different regimes of pool boiling of water. The temperature of the wire was determined from the knowledge of the manner in which its electrical resistance varied with temperature. [Ref. 10].

A. SEM ANALYSIS OF PLATINUM WIRE

The platinum wire, from the same sample which is used during the experiments, is analyzed in Scanning Electron Microscope under two magnifications. The magnification of 666x, as it can be seen in Figure 14a, yields that the diameter of the platinum wire is 0.05113mm. The magnification of 1270x (Figure 14b) shows the lengthwise line formations created during the manufacturing process. The surface of the wire is relatively smooth in appearance with the exception of one raised ridge line extending the length of the sample. Several small surface defects of approximately 1-2 μm are diameters are present on the surface of the wire. The defects are dispersed throughout the surface of the wire. These are possible nucleation sites for nucleate boiling.

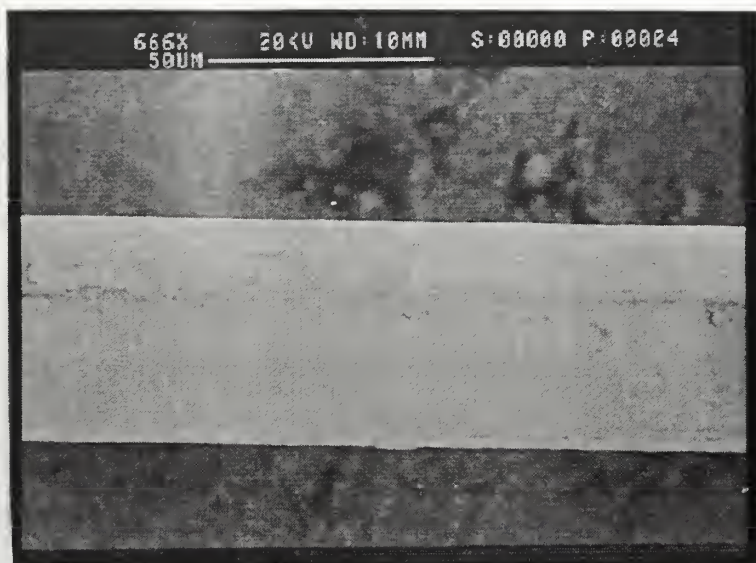


Figure 14a. SEM Picture of Sample Platinum Wire (666x).

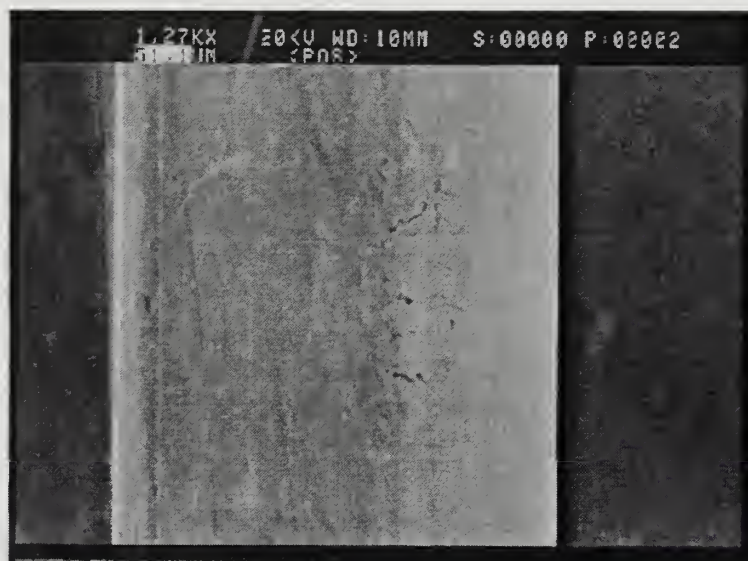


Figure 14b. SEM Picture of Sample Platinum Wire (1270x).

B. CALIBRATION PROCEDURE IN THE CALIBRATION BATH

During the calibration in the bath the following equipment was used:

1. HP 3852A Data Acquisition System with installed Ohmmeter.
2. Rosemont Engineering Company Model 162C Serial No. 985 Platinum Resistance Thermometer (PRT) (to measure the calibration bath temperature. According to Reference 11, PRT has been calibrated in comparison with a platinum resistance temperature standard, which is done by the National Bureau of Standards.)
3. Rosemont Engineering Company Model 923B Power Supply (to control bath temperature with Neslab Endocal Refrigerated circulation bath)
4. Rosemont Engineering Company Model 920A Commutating Bridge (to measure PRT resistance for temperature measurement)
5. Rosemont Engineering Company Model 913A Calibration Bath (fluid in the bath is ethylene glycol)

The 0.05 mm platinum wire has been mounted on a Plexiglas board and the spring assembly applies tension in order to keep the wire straight throughout the calibration process. The board and spring assembly is immersed into the Rosemont Engineering constant temperature bath. The platinum wire is electrically connected to the HP 3852A Data Acquisition System. The Data Acquisition System will use an internal ohmmeter to measure the resistance of the wire during the procedure. First the line resistance of the platinum wire is measured. The temperature of the bath will be increased from 20°C to 85°C with increments of 5°C. When the bath temperature reaches steady state at each temperature increment, the resistance of the platinum wire and the bath temperature is

recorded. Once the data is recorded at 85°C, the process is repeated using temperature decrements of 10°C until 20°C is achieved. The bath temperature and platinum wire resistance are measure again at each interval once steady state is achieved. The measurements are recorded during the temperature decrements in order to detect possible hysteresis in measurements.

C. CALIBRATION PROCEDURE IN THE MAIN CHAMBER

After the platinum wire is placed in the main chamber and the chamber is filled with FC-72, another calibration procedure was conducted prior to securing the heat exchanger to the top of the main chamber. The procedure will use the same equipment as in Part B with the exception of the calibration bath and power supply. The FC-72 will be heated in the main chamber by the installed strip heaters. The temperature of the FC-72 will start at 20 °C and will rise in 5 °C increments until saturation temperature of 56 °C is achieved.

D. RESULTS AND ERROR ANALYSIS FOR CALIBRATION

The calibration data from the test run in the calibration bath is displayed in Table 4 and the plot shown in Figure . The curve fitting of the acquired data resulted in the following equation;

$$T_{\text{surf}} = 49.689 \bullet R_{\text{Pt.Wire}} - 253.836$$

Where: T_{surf} = Surface temperature of the platinum wire in °C.

$R_{\text{Pt.Wire}}$ = Resistance of the platinum wire in Ohms.

The platinum wire was again calibrated upon the completion of the experiments to verify proper operation. The resulting calibration curve produced higher temperature values for a given wire resistance. This change in the calibration results could be due aging in the

platinum wire created by the cyclic thermal stresses imposed on the wire during the experiments. The resulting calibration curve data is given in Table 7 and a graph of both calibration curves is Figure 18.

Resistance (Ohms)	Temperature (°C)	Temperature 1 (°C)	Percent Error (%)
5.533	21.12	21.09	0.1421
5.6185	25.35	25.34	0.3290
5.749	30.46	31.83	4.480
5.812	34.97	35.11	0.3870
5.924	40.58	40.35	0.5667
6.027	45.69	45.63	0.1103
6.129	50.74	50.71	0.0630
6.240	56.73	56.22	0.8930
6.342	61.34	61.29	0.0788
6.437	66.01	66.59	0.8780
6.536	70.45	70.93	0.6830
6.636	75.93	75.50	0.5663
6.721	80.14	80.12	0.0202
6.835	85.51	85.79	0.3270
6.643	76.31	76.21	0.1310
6.427	65.54	65.51	0.0378
6.234	55.98	55.82	0.0978
6.006	44.63	44.49	0.3140
5.818	35.38	35.25	0.3540
5.615	25.17	25.16	0.0397

Table 4. Calibration Data and Linear Aggression Results.

Resistance (Ohms)	Temperature (°C)
5.631	21.71
5.693	24.90
5.776	28.30
5.834	31.65
5.917	35.931
5.943	37.24
5.968	38.49
5.985	39.145
6.008	40.587
6.072	43.718
6.129	46.277
6.157	47.665
6.168	48.687
6.230	51.77
6.280	54.268
6.289	54.755
6.293	55.019

Table 5. In-Place Calibration.

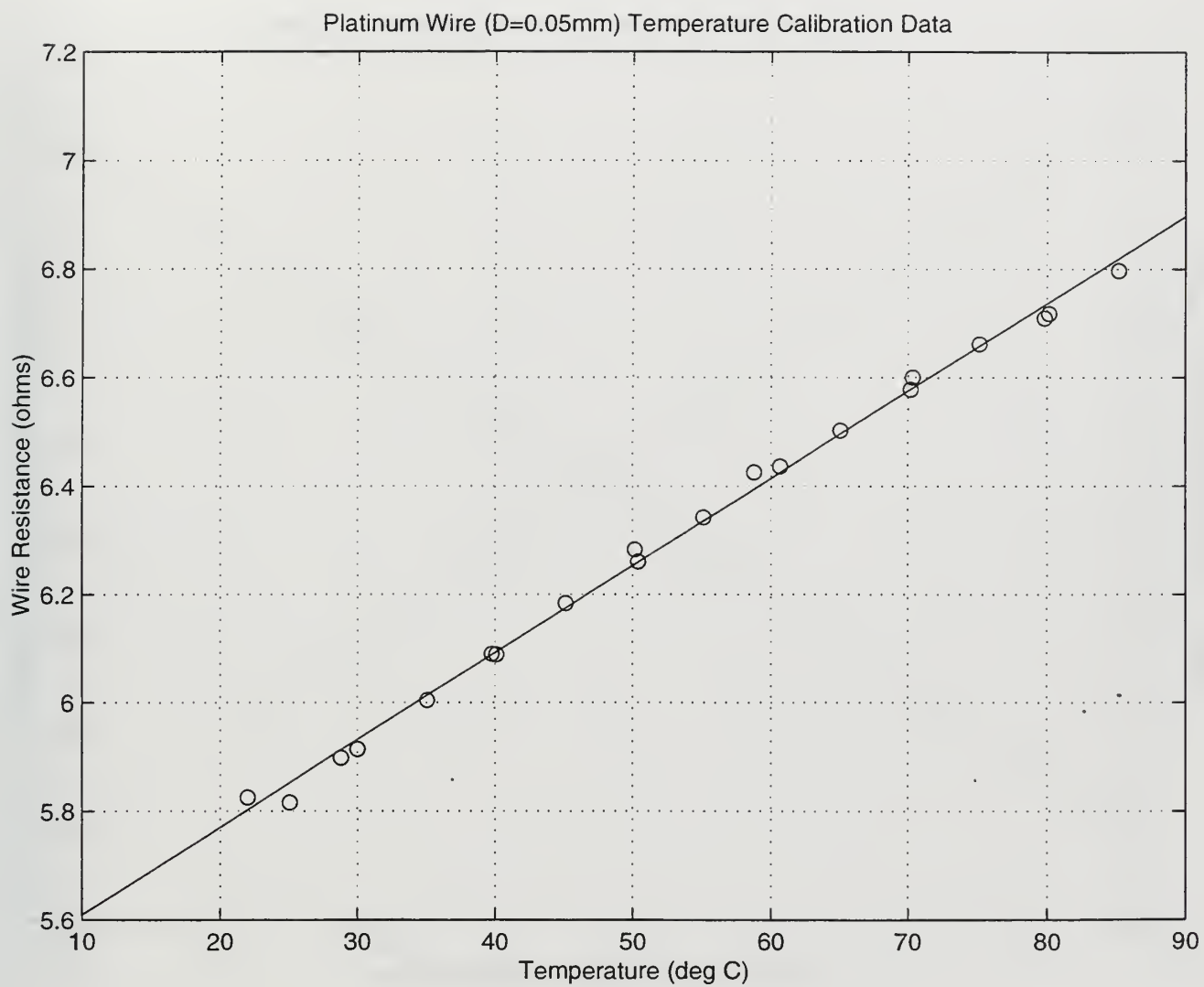


Figure 15. Calibration Curve of Platinum Wire.

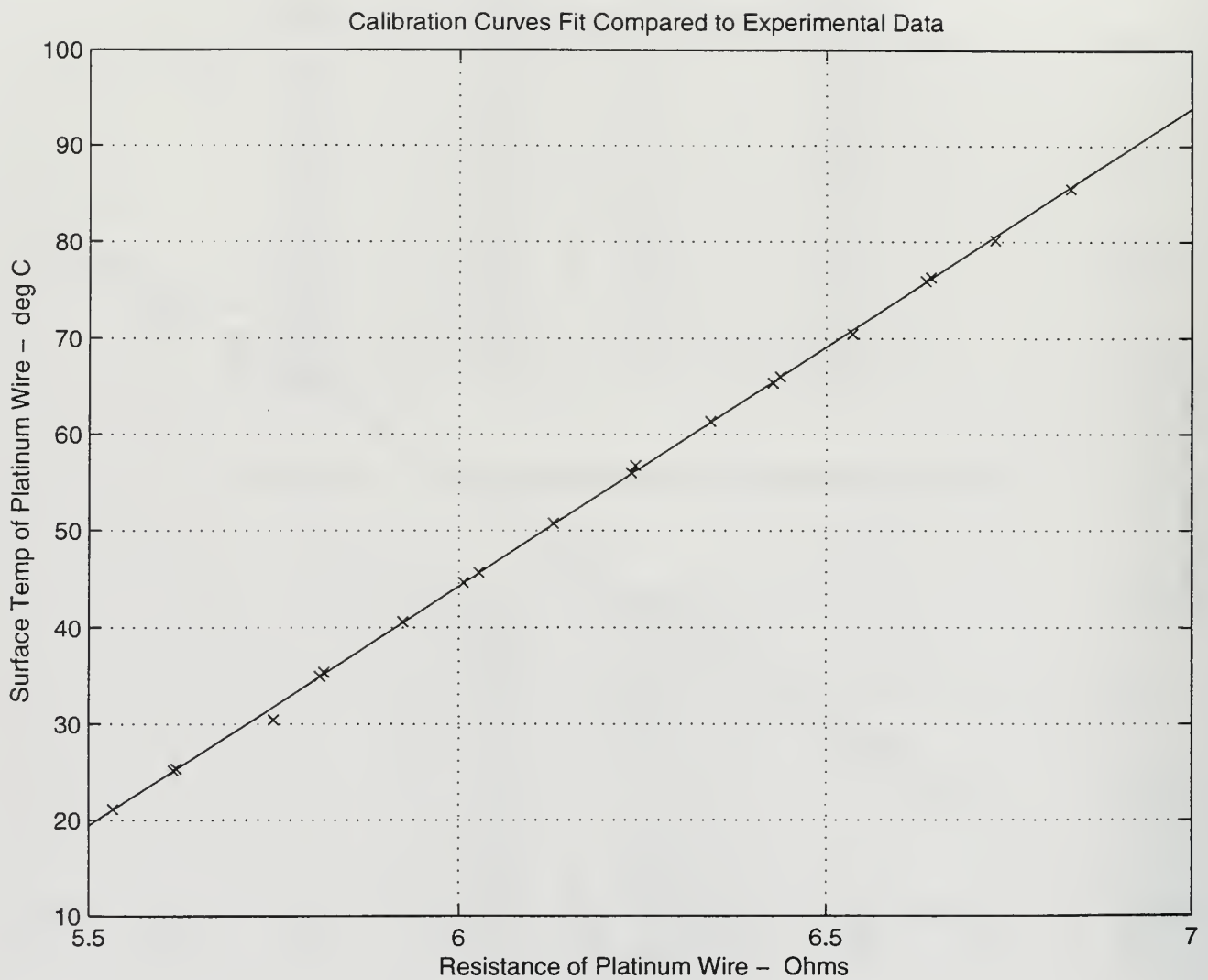


Figure 16. Calibration Curve Fit Compared to Experimental Data.

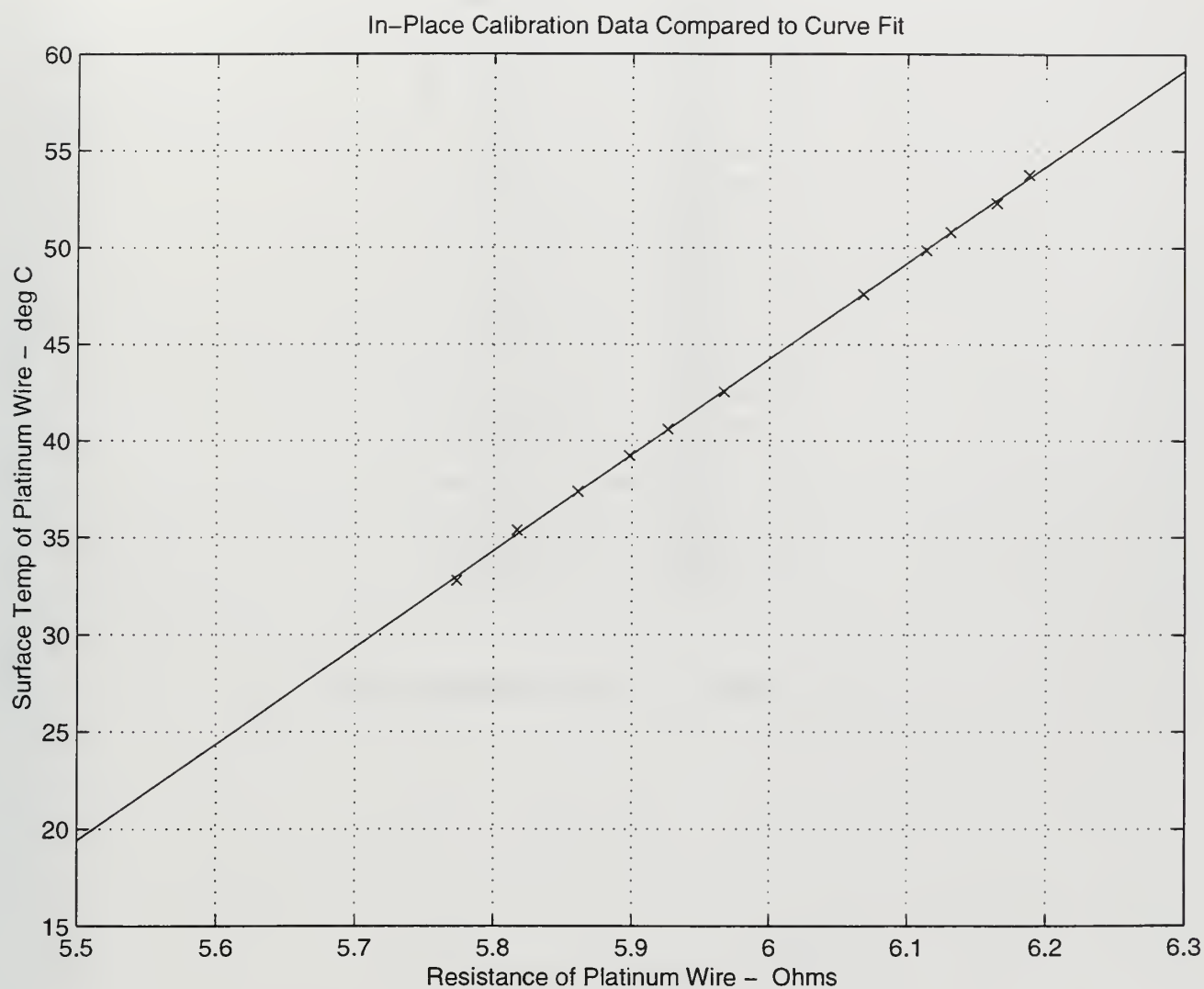


Figure 17. In-Place Calibration Data Compared to Calibration Curve Fit.

Resistance (Ohms)	Temperature (°C)
5.439	22.35
5.590	30.13
5.721	36.48
5.825	41.69
6.00	50.48
6.097	55.33
6.228	61.91
6.289	65.01
6.387	69.98
6.477	74.48
6.565	79.63
6.694	85.11
6.593	80.13
6.399	70.46
6.2085	60.75
6.01	51.09
5.841	42.13
5.625	31.56
5.423	21.55

Table 6. Final Calibration Data

Final Calibration Curve

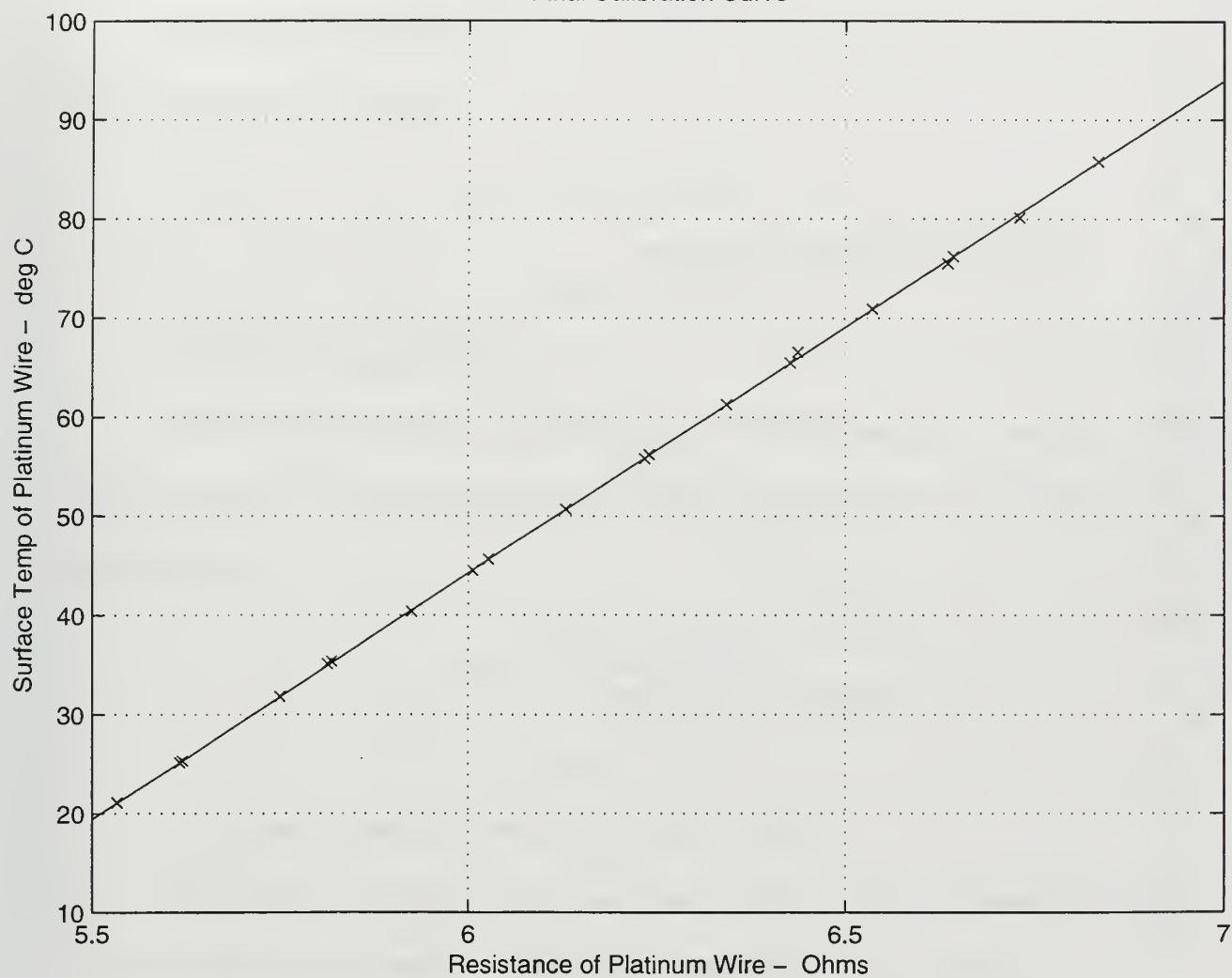


Figure 18. Final Calibration Curve.

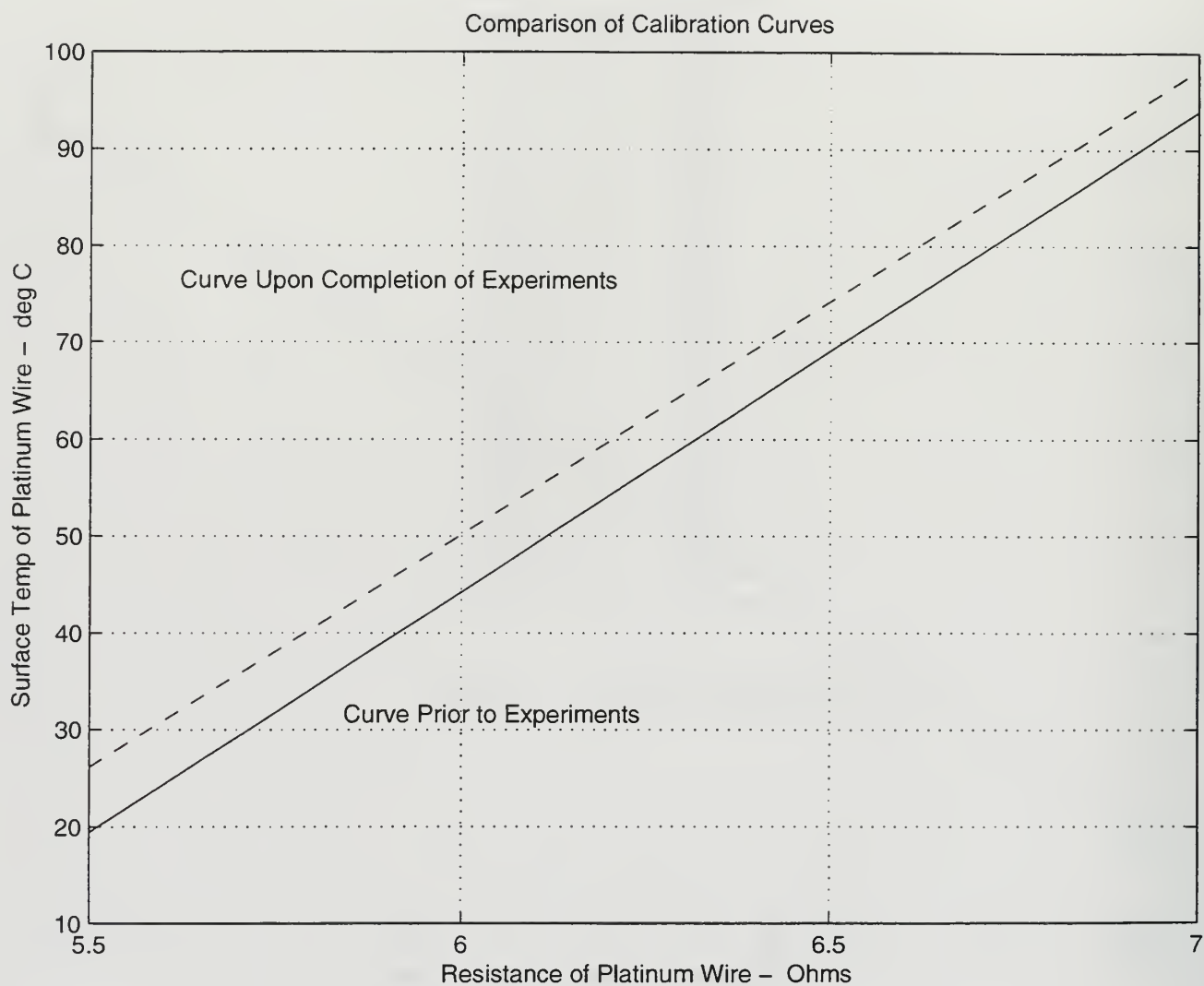


Figure 19. Comparison of Calibration Curves.

APPENDIX B. SAMPLE CALCULATIONS

A. DETERMINATION OF EXPERIMENTAL VALUES

The following sample calculations are the results of the 6th experiment. This experiment is the boiling curve of FC-72.

1. Condenser temperature:

The condenser temperature is the average of four thermocouples in the region of the condenser/heat exchanger.

$$T_{\text{cond}} = \frac{(T_0 + T_1 + T_2 + T_3)}{4}$$

$$T_{\text{cond}} = 27.123^{\circ}\text{C}$$

2. Fluid bulk temperature:

The fluid temperature is the average of four thermocouple readings. The thermocouples are located inside the main chamber approximately one inch below the platinum wire.

$$T_{\text{bulk}} = \frac{(T_4 + T_5 + T_6 + T_7)}{4}$$

$$T_{\text{bulk}} = 53.343^{\circ}\text{C}$$

3. Current of platinum wire and precision resistor:

The current of the platinum wire and the precision resistor is obtained from the division of the voltage drop across the precision resistor divided by its resistance value.

$$I_{\text{Pt. Wire}} = I_{2\Omega} = \frac{V_{2\Omega}}{R_{2\Omega}}$$

$$I_{\text{Pt. Wire}} = I_{2\Omega} = \frac{0.465}{2.03} = 0.2282\text{A}$$

4. Platinum wire resistance value:

The platinum wire resistance is obtained from the division of the voltage drop across the platinum wire by the platinum wire current.

$$R_{Pt.Wire} = \frac{V_{Pt.Wire}}{I_{Pt.Wire}}$$

$$R_{Pt.Wire} = \frac{1.4429}{0.2282}$$

$$R_{Pt.Wire} = 6.3234 \Omega$$

5. Platinum wire surface temperature:

To find the platinum wire surface temperature, the calibration formula in the APPENDIX A is used with the platinum wire resistance as an input.

$$T_{surf} = 49.689 \cdot R_{pt.Wire} - 253.836$$

$$T_{surf} = (49.689 \cdot 6.3234) - 253.836$$

$$T_{surf} = 60.367 \text{ }^{\circ}\text{C}$$

6. Heat flux from platinum wire:

The heat flux from the platinum wire is equal to the division of electrical power supplied to the platinum wire by the platinum wire surface area.

$$Q'' = \frac{I_{Pt.Wire} \cdot V_{Pt.Wire}}{A_{Pt.Wire}}$$

$$Q'' = \frac{0.2282 \cdot 1.4429}{1.76025 \cdot 10^{-5}}$$

$$Q'' = 18,709.12 \text{ W/m}^2$$

Where $A_{Pt.Wire} = \pi \cdot L_{Pt.Wire} \cdot D_{Pt.Wire}$

$$A_{Pt.Wire} = \pi \cdot 0.1018736 \cdot 5.112 \cdot 10^{-6} = 1.635 \cdot 10^{-6} \text{ m}^2$$

7. Piston displacement:

The piston displacement is equal to the cross sectional area multiplied by the piston stroke length. The following calculations in parts 7 and 8 are done for the stroke length of 13.3 mm.

$$\Delta_{Piston} = \frac{\pi}{4} \cdot D_{Piston}^2 \cdot L_{Stroke}$$

$$\Delta_{Piston} = \frac{\pi}{4} \cdot (9.525)^2 \cdot 13.3$$

$$\Delta_{Piston} = 947.701 \text{ mm}^3$$

8. Amplitude of oscillation in the main chamber:

The amplitude of the oscillation in the main chamber is obtained from the division of piston displacement by the main chamber cross sectional area.

$$A_{Amplitude} = \frac{\Delta_{Piston}}{a \cdot b}$$

Where a and b are the inner dimensions of the main chamber

$$A_{Amplitude} = \frac{947.701}{152.2984 \cdot 59.377}$$

$$A_{Amplitude} = 0.105 \text{ mm}$$

9. Frequency calculation:

The frequency of the oscillation is the arithmetical inverse of the oscillation period reading in seconds. The following calculation is completed for a frequency of 1.2 Hz.

$$F = \frac{1}{T_{Period}(s)} = \frac{1}{0.8333} = 1.2 \text{ Hz}$$

B. DETERMINATION OF NUMERICAL VALUES

In this part, natural convection heat transfer around the platinum wire immersed in FC-72 is calculated numerically by using recommended correlation by Kuehn and Goldstein [Ref. 3] and Egger's results [Ref. 9] are used for fluid properties.

1. Film temperature:

$$T_{\text{film}} = \frac{(T_{\text{bulk}} + T_{\text{Pt.Wire}})}{2}$$

$$T_{\text{film}} = \frac{(53.343 + 60.367)}{2}$$

$$T_{\text{film}} = 56.855 \text{ }^{\circ}\text{C}$$

2. Thermal conductivity:

$$K = \frac{(0.6033 - 0.00115 \cdot T_{\text{film}})}{10.0}$$

$$K = 0.05379 \text{ W/m }^{\circ}\text{C}$$

3. Liquid density:

$$\rho_l = (1.740 - 0.00261 \cdot T_{\text{film}}) \cdot 1000$$

$$\rho_l = 1.5916 \cdot 10^3 \text{ kg/m}^3$$

4. Kinematic viscosity:

$$\nu = 1.203952 \cdot 10^{-8} \cdot \exp\left(\frac{1058.4109}{T_{\text{film}} + 273.15}\right)$$

$$\nu = 0.29832 \cdot 10^{-6} \text{ m}^2/\text{sec}$$

5. Specific heat:

$$C_p = (0.241111 + 3.70337 \cdot 10^{-4} \cdot T_{\text{film}}) \cdot 4186$$

$$C_p = 1.09742 \cdot 10^3 \text{ J/kg }^{\circ}\text{C}$$

6. Thermal expansion coefficient:

$$\beta = \frac{0.00261}{(1.740 - 0.00261 \cdot T_{film})}$$

$$\beta = 0.0016398 \text{ } 1/^{\circ}\text{C}$$

7. Thermal diffusivity:

$$\alpha = \frac{k}{\rho_l \cdot C_p}$$

$$\alpha = 0.31041 \cdot 10^{-7} \text{ m}^2/\text{sec}$$

8. Prandtl number:

$$\text{Pr} = \frac{\nu}{\alpha}$$

$$\text{Pr} = 9.6105$$

9. Rayleigh number:

$$\text{Ra}_D = \frac{g \cdot B \cdot (T_{Pt.Wire} - T_{bulk})}{\nu \cdot \alpha} \cdot D_{Pt.Wire}^3$$

$$\text{Ra}_D = 1.502$$

10. Nusselt number:

$$\text{Nu}_D = \frac{2}{\log \left[1 + \frac{2}{\left[\left(0.518 \cdot \text{Ra}_D^{1/4} \cdot \left[1 + \left(\frac{0.559}{\text{Pr}} \right)^{3/5} \right]^{-5/12} \right)^{15} + \left(0.1 \cdot \text{Ra}_D^{1/3} \right)^{1/15} \right]} \right]}$$

$$\text{Nu}_D = 1.579$$

11. Heat flux:

$$Q'' = \frac{k \cdot Nu_D \cdot (T_{Pt.Wire} - T_{bulk})}{D}$$

$$Q'' = 11,640 \text{ W/m}^2$$

APPENDIX C. UNCERTAINTY ANALYSIS

A. UNCERTAINTY IN SURFACE AREA

$$D_{Pt.Wire} = 51.1\mu m = 0.0511mm \quad \text{Wire Diameter}$$

$$L_{Pt.Wire} = 4.051in = 102.8mm \quad \text{Wire Length}$$

$$\omega_D = 0.002mm \quad \text{Uncertainty in Wire Diameter}$$

$$\omega_L = 0.06in = 1.52mm \quad \text{Uncertainty in Wire Length}$$

$$A_{Pt.Wire} = \pi \cdot L_{Pt.Wire} \cdot D_{Pt.Wire} \quad \text{Wire Surface Area}$$

$$A_{Pt.Wire} = \pi \cdot 0.1028m \cdot 5.11 \cdot 10^{-6}m$$

$$A_{Pt.Wire} = 1.65 \cdot 10^{-5} m^2$$

$$\frac{\partial A_{Pt.Wire}}{\partial D_{Pt.Wire}} = (\pi \cdot L_{Pt.Wire})$$

$$\frac{\partial A_{Pt.Wire}}{\partial L_{Pt.Wire}} = (\pi \cdot D_{Pt.Wire})$$

Then the uncertainty in surface area is:

$$\omega_{A,Pt.Wire} = \sqrt{(\pi \cdot L_{Pt.Wire} \cdot \omega_D)^2 + (\pi \cdot D_{Pt.Wire} \cdot \omega_L)^2}$$

$$\frac{\omega_{A,Pt.Wire}}{A_{Pt.Wire}} = \sqrt{\left(\frac{\omega_D}{D_{Pt.Wire}}\right)^2 + \left(\frac{\omega_L}{L_{Pt.Wire}}\right)^2}$$

$$\frac{\omega_{A,Pt.Wire}}{A_{Pt.Wire}} = \sqrt{\left(\frac{0.002}{0.0511}\right)^2 + \left(\frac{1.524}{102.8}\right)^2}$$

$$\frac{\omega_{A,Pt.Wire}}{A_{Pt.Wire}} = 0.0418 \text{ or } 4.18\%$$

$$\omega_{A,Pt.Wire} = 6.91 \cdot 10^{-7} m^2$$

B. UNCERTAINTY IN POWER

$$\omega_{V,2\Omega} = 0.006\% \quad \text{Uncertainty in Precision Resistor Voltage Drop [Ref. 11]}$$

$$\omega_{V,Pt.Wire} = 0.006\% \quad \text{Uncertainty in Platinum Wire Voltage Drop [Ref. 11]}$$

$$\omega_{R,2\Omega} = 0.02\% \quad \text{Uncertainty in Precision Resistor}$$

$$Q = V_{Pt.Wire} \cdot I_{Pt.Wire}$$

$$Q = V_{Pt.Wire} \cdot \frac{V_{2\Omega}}{R_{2\Omega}}$$

$$\frac{\partial Q}{\partial V_{Pt.Wire}} = \left(\frac{V_{2\Omega}}{R_{2\Omega}} \right)$$

$$\frac{\partial Q}{\partial V_{2\Omega}} = \left(\frac{V_{Pt.Wire}}{R_{2\Omega}} \right)$$

$$\frac{\partial Q}{\partial R_{2\Omega}} = \left(\frac{-V_{Pt.Wire} \cdot V_{2\Omega}}{R_{2\Omega}^2} \right)$$

Then the uncertainty in power is:

$$\omega_Q = \sqrt{\left(\frac{V_{2\Omega}}{R_{2\Omega}} \cdot \omega_{V,Pt.Wire} \right)^2 + \left(\frac{V_{Pt.Wire}}{R_{2\Omega}} \cdot \omega_{V,2\Omega} \right)^2 + \left(\frac{-V_{Pt.Wire} \cdot V_{2\Omega}}{R_{2\Omega}^2} \cdot \omega_{R,2\Omega} \right)^2}$$

$$\frac{\omega_Q}{Q} = \sqrt{\left(\frac{\omega_{V,Pt.Wire}}{V_{Pt.Wire}} \right)^2 + \left(\frac{\omega_{V,2\Omega}}{V_{2\Omega}} \right)^2 + \left(\frac{\omega_{R,2\Omega}}{R_{2\Omega}} \right)^2}$$

$$\frac{\omega_Q}{Q} = \sqrt{\left(\frac{0.006\%}{100} \right)^2 + \left(\frac{0.006\%}{100} \right)^2 + \left(\frac{0.02}{2.03} \right)^2}$$

$$\frac{\omega_Q}{Q} = 0.099 \text{ or } 0.99\%$$

C. UNCERTAINTY IN HEAT FLUX

$$Q'' = \frac{Q}{A_{Pt.Wire}}$$

$$\frac{\partial Q''}{\partial Q} = \left(\frac{1}{A_{Pt.Wire}} \right)$$

$$\frac{\partial Q''}{\partial A} = \left(\frac{-Q}{A_{Pt.Wire}^2} \right)$$

Then the uncertainty in heat flux is:

$$\omega_{Q''} = \sqrt{\left(\frac{-Q}{A_{Pt.Wire}^2} \cdot \omega_A \right)^2 + \left(\frac{1}{A_{Pt.Wire}} \cdot \omega_Q \right)^2}$$

$$\frac{\omega_{Q''}}{Q''} = \sqrt{\left(\frac{\omega_A}{A} \right)^2 + \left(\frac{\omega_Q}{Q} \right)^2}$$

$$\frac{\omega_{Q''}}{Q''} = \sqrt{(0.0418)^2 + (0.0099)^2}$$

$$\frac{\omega_{Q''}}{Q''} = 0.0429 \text{ or } 4.29\%$$

D. UNCERTAINTY IN TEMPERATURE

The uncertainty in the thermocouple temperature measurements is the sum of the uncertainties due to the hardware and software, namely HP 3852A and the software used in this study. According to Ref. 11, the temperature measurement accuracy with the HP 3852A Data Acquisition System is $\pm 0.4^\circ\text{C}$ in the temperature range of 0 to 300°C .

$$\omega_{TC} = 0.4^\circ\text{C}$$

E. UNCERTAINTY IN WIRE SURFACE TEMPERATURE

As it is given in Appendix A, Section C ‘Results and Error Analysis’ maximum uncertainty is:

$$\frac{\omega_{T_{surf}}}{T_{surf}} = 3.031\%$$

$$\omega_{T_{surf}} = 0.8696^{\circ}\text{C} \quad \text{For the surface temperature of } 28.69^{\circ}\text{C}.$$

F. UNCERTAINTY IN OSCILLATION AMPLITUDE

$$D_{\text{Piston}} = 9.25\text{mm}$$

$$L_{\text{Stroke}} = 10\text{mm}$$

$$A = 102.1\text{mm}$$

$$B = 60.2\text{mm}$$

$$\omega_{D,\text{Piston}} = 0.002\text{mm}$$

$$\omega_{L,\text{Piston}} = 0.5\text{mm}$$

$$\omega_a = 0.25\text{mm}$$

$$\omega_b = 0.25\text{mm}$$

$$A_{\text{Amplitude}} = \frac{\pi}{4} \cdot \frac{D_{\text{Piston}}^2 \cdot L_{\text{Stroke}}}{a \cdot b}$$

$$\frac{\partial A_{\text{Amplitude}}}{\partial D_{\text{Piston}}} = \left(\frac{\pi}{2} \cdot \frac{D_{\text{Piston}} \cdot L_{\text{Stroke}}}{a \cdot b} \right)$$

$$\frac{\partial A_{\text{Amplitude}}}{\partial L_{\text{Piston}}} = \left(\frac{\pi}{4} \cdot \frac{D_{\text{Piston}}^2}{a \cdot b} \right)$$

$$\frac{\partial A_{\text{Amplitude}}}{\partial a} = \left(\frac{\pi}{4} \cdot \frac{D_{\text{Piston}}^2 \cdot L_{\text{Stroke}}}{b} \cdot \left(\frac{-1}{a^2} \right) \right)$$

$$\frac{\partial A_{Amplitude}}{\partial b} = \left(\frac{\pi}{4} \cdot \frac{D_{Piston}^2 \cdot L_{Stroke}}{a} \cdot \left(\frac{-1}{b^2} \right) \right)$$

$$\omega_{A,Amp} = \sqrt{\left(\omega_{Dpis} \cdot \frac{\pi}{2} \cdot \frac{D_{Pis} \cdot L_{Str}}{a \cdot b} \right)^2 + \left(\omega_{Lpis} \cdot \frac{\pi}{4} \cdot \frac{D_{Pis}^2}{a \cdot b} \right)^2 + \left(\omega_a \cdot \frac{\pi}{4} \cdot \frac{D_{Pis}^2 \cdot L_{Str}}{b} \cdot \left(\frac{-1}{a^2} \right) \right)^2 + \left(\omega_b \cdot \frac{\pi}{4} \cdot \frac{D_{Pis}^2 \cdot L_{Str}}{a} \cdot \left(\frac{-1}{b^2} \right) \right)^2}$$

$$\frac{\omega_{A,Amplitude}}{A_{Amplitude}} = \sqrt{\left(\frac{\omega_{DPiston}}{2 \cdot D_{Piston}} \right)^2 + \left(\frac{\omega_{LStroke}}{L_{Stroke}} \right)^2 + \left(\frac{\omega_a}{a} \right)^2 + \left(\frac{\omega_b}{b} \right)^2}$$

$$\frac{\omega_{A,Amplitude}}{A_{Amplitude}} = \sqrt{\left(\frac{0.005}{2 \cdot 9.525} \right)^2 + \left(\frac{0.5}{10} \right)^2 + \left(\frac{0.01}{152.1} \right)^2 + \left(\frac{0.01}{60.2} \right)^2}$$

$$\frac{\omega_{A,Amplitude}}{A_{Amplitude}} = 0.0506 \text{ or } 5.06\%$$

G. UNCERTAINTY IN OSCILLATION FREQUENCY

Because of the friction factor uncertainty in the frequency is higher at the lower frequencies:

$$T_{Period} = 2.5 \text{ sec}$$

$$\omega_{T,Period} = 0.05 \text{ sec}$$

$$f = \frac{1}{T_{Period}}$$

$$\frac{\omega_f}{f} = \frac{\omega_{T,Period}}{T_{Period}}$$

$$\frac{\omega_f}{f} = 0.02 \text{ or } 2\%$$



APPENDIX D. COMPUTER PROGRAM

This program will be used for data reduction. It will take the acquired data from the experimental apparatus and calculate the heat flux and temperature overshoot. The heat flux as calculated by the natural convection heat transfer correlation will also be plotted and compared to the experimental results.

Data Reduction Program During the Experiment

This part of the program will take the raw data, correct the temperatures using the calibration equations, and send the data into the main part of the program.

C = [-0.0001 1.0058 -0.0199;

-0.0001 1.0072 -0.0493;

-0.0001 1.0068 -0.0572;

-0.0001 1.0073 -0.0509;

-0.0000 1.0047 -0.0028;

-0.0001 1.0070 -0.0523;

-0.0001 1.0077 -0.0583;

-0.0001 1.0089 -0.0797;

-0.0001 1.0073 -0.0540;

-0.0001 1.0062 -0.0471;

-0.0002 1.0158 -0.1899;

-0.0001 1.1186 -0.0809;

0.0000 1.0000 0.0000;

0.0000 1.0000 0.0000];

```

for j = 1:35
    if (j==1)
        load run01
        t=run01;
    end;
    if (j==2)
        load run02
        t=run02;
    end;
    if (j==3)
        load run03
        t=run03;
    end;
    if (j==4)
        load run04
        t=run04;
    end;
    if (j==5)
        load run05
        t=run05;
    end;
    if (j==6)
        load run06
        t=run06;
    end;
    if (j==7)
        load run07
        t=run07;
    end;
    if (j==8)
        load run08
        t=run08;
    end;
    if (j==9)
        load run09
        t=run09;
    end;
    if (j==10)
        load run10
        t=run10;
    end;
    if (j==11)
        load run11
        t=run11;
    end;
    if (j==12)

```

```

        load run12
        t=run12;
    end;
        if (j==13)
            load run13
            t=run13;
        end;
        if (j==14)
            load run14
            t=run14;
        end;
        if (j==15)
            load run15
            t=run15;
        end;
        if (j==16)
            load run16
            t=run16;
        end;
        if (j==17)
            load run17
            t=run17;
        end;
        if (j==18)
            load run18
            t=run18;
        end;
        if (j==19)
            load run19
            t=run19;
        end;
        if (j==20)
            load run20
            t=run20;
        end;
        if (j==21)
            load run21
            t=run21;
        end;
        if (j==22)
            load run22
            t=run22;
        end;
        if (j==23)
            load run23
            t=run23;

```

```
end;  
    if (j==24)  
        load run24  
        t=run24;  
end;  
    if (j==25)  
        load run25  
        t=run25;  
end;  
    if (j==26)  
        load run26  
        t=run26;  
end;  
    if (j==27)  
        load run27  
        t=run27;  
end;  
    if (j==28)  
        load run28  
        t=run28;  
end;  
    if (j==29)  
        load run29  
        t=run29;  
end;  
    if (j==30)  
        load run30  
        t=run30;  
end;  
    if (j==31)  
        load run31  
        t=run31;  
end;  
    if (j==32)  
        load run32  
        t=run32;  
end;  
    if (j==33)  
        load run33  
        t=run33;  
end;  
    if (j==34)  
        load run34  
        t=run34;  
end;
```

```

        if (j==35)
        load run35
        t=run35;
    end;

    for i = 1:14

        T(i,j) = C(i,1)*t(i)^2 + C(i,2)*t(i) + C(i,3);

    end;

end;

```

This part of the program will be used in data reduction for the experiment.

First the data is loaded into the active part of the program.

```

Q = zeros(1,35);
Tsh = Q;

for j = 1:35

```

The first calculation will be to determine the temperature of the condenser.

```

    Temp = T(:,j);

    Tc = mean(Temp(1:4));

```

Next the temperature of the bulk fluid will be calculated.

```

    Tb(j) = mean(Temp(5:7));

```

The voltage drop will be used to find Resistance of Platinum wire.

```

    Vr(j) = Temp(13);

    Vp(j) = Temp(14);

    Ic(j) = Vr(j)/2.03;

    Ip(j) = Ic(j);

```

$$R_p(j) = V_p(j)/I_p(j);$$

The resistance of the platinum wire will be used to calculate the actual surface temperature of the platinum wire.

$$T_{surf}(j) = 49.989 * R_p(j) - 253.847;$$

The film temperature of the fluid in direct contact with the wire is calculated using the surface temperature and the bulk temperature.

$$T_{film}(j) = (T_{surf}(j) + T_b(j))/2;$$

The wall superheat needs to be calculated. This value is a measure of the temperature difference between the platinum wire and the saturation temperature of the FC-72.

$$T_{sh}(j) = T_{surf}(j) - 56.1;$$

The heat flux generated by the wire is calculated based on the power output of the wire and its area.

$$Q(j) = (I_p(j) * V_p(j))/1.76025e-5;$$

The two values that need to be saved from each data run are the heat flux Q and the wall superheat T_{sh} .

This part of the program will calculate the natural convection heat flux based on the Kuehn and Goldstein correlation.

if $j \leq 8$

Thermal conductivity calculation. (W/cm^2)

$$k = ((0.6033 - 0.00115 * T_{film}(j))/10);$$

Liquid density calculation. (kg/m^3)

$$\rho = (1.74 - 0.00261 * T_{film}(j)) * 1000;$$

Kinematic viscosity calculation. (m^2/sec)

$$\nu = ((1.203952e-08) * (\exp(1058.4109/(T_{film}(j)+273))));$$

Specific heat calculation. ($J/kg\ C$)

$$C_p = (0.241111 + 3.70337e-04 * T_{film}(j)) * 4186;$$

Thermal expansion coefficient. (1/ C)

$$B = 0.00261/(1.740 - 0.00251 * T_{\text{film}}(j));$$

Thermal diffusivity.

$$\alpha = k/(p * C_p);$$

Prandtl number.

$$Pr = \nu / \alpha;$$

Rayleigh number.

$$Ra(j) = (9.817 * B * (T_{\text{surf}}(j) - T_b(j)) * (0.05e-03)^3) / (\nu * \alpha);$$

Nusselt number.

$$Nu(j) = 2 / \log(1 + (2 / ((0.518 * Ra(j)^{0.25} * (1 + (0.559 / Pr)^{0.6})^{-0.4167})^{15} + (0.1 * Ra(j)^{0.333})^{15})^{0.0667}));$$

Heat flux.

$$q(j) = k * Nu(j) * (T_{\text{surf}}(j) - T_b(j)) / 0.05e-03;$$

else

$$z(j) = 0;$$

end

end;

This part of the program will reorganize the data and prepare it to be graphed and displayed so the values can be compared to one another.

$$KG = T_{\text{sh}}(1:8);$$

$$KGQ = Q(1:8);$$

$$Tb1 = T_b(1:22); \quad Tb2 = T_b(22:35);$$

$$T1 = T_{\text{sh}}(1:22); \quad T2 = T_{\text{sh}}(22:35);$$

$$Q1 = Q(1:22); \quad Q2 = Q(22:35);$$

```

format short e
semilogy(T1,Q1,'x',T1,Q1,'-',T2,Q2,'o',T2,Q2,'-
',KG,q,'x',KG,q,'.',Tb1,Q1,'+',Tb2,Q2,'.'),grid;
axis([0,90,10000,1000000]);
title('Heat flux vs. Wall superheat');
xlabel('Wall Superheat deg C');
ylabel('Wire Heat Flux W/cm^2');

```

This part of the program will display the two heat flux values and the temperature overshoot value.

```

Final = ([Q',Tsh'])
Flux = ([KGQ',KG',q'])

```

This will save the graph to a file for easy printout later.

```

print -dps2 plot1

```

APPENDIX E. EXPERIMENTAL DATA

A. EXPERIMENTAL DATA

1. The results of each experimental run are displayed in Table 6. Most experimental runs, which were not completed, were halted due to leaks developing in the main chamber. The highly wetting FC-72 was able to seep through the seams of the main and front chambers. Re-applying silicon sealant after each set of experiments to seams of main chamber halted the leaks.

2. Figures 20 – 32 are the heat flux vs. wall superheat plots from the experimental runs that were not displayed in Chapter IV.

Experiment	Results
1	Stopped -- leaks
2	Stopped -- leaks
3	Stopped -- broken wire leading to power supply
4	Completed
5	Stopped -- leaks
6	Completed
7	Stopped -- pump failed
8	Stopped -- leaks
9	Stopped -- leak in heat exchanger
10	Stopped -- leaks
11	Stopped -- incorrect piston stroke length
12	Completed
13	Completed
14	Completed
15	Completed
16	Completed
17	Completed
18	Completed
19	Completed
20	Completed
21	Completed
22	Completed
23	Completed
24	Completed
25	Completed
26	Completed
27	Completed
28	Completed
29	Completed
30	Stopped -- leaks
31	Stopped -- leaks
32	Stopped -- leaks

Table 7. Status of Experimental Runs.

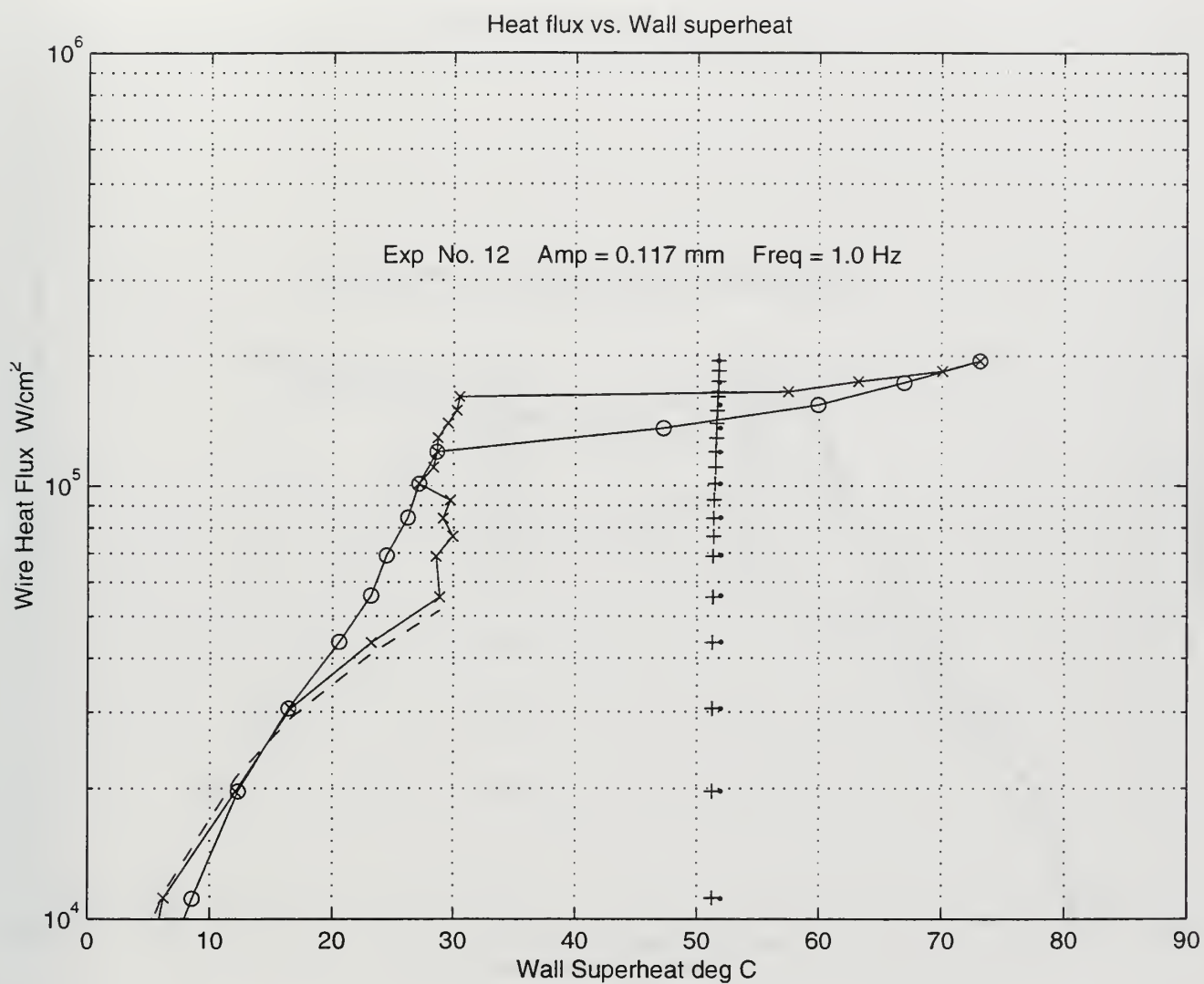


Figure 20. Boiling Curve of FC-72 with an Oscillation of Amplitude 0.117mm and a Frequency of 1.0Hz.

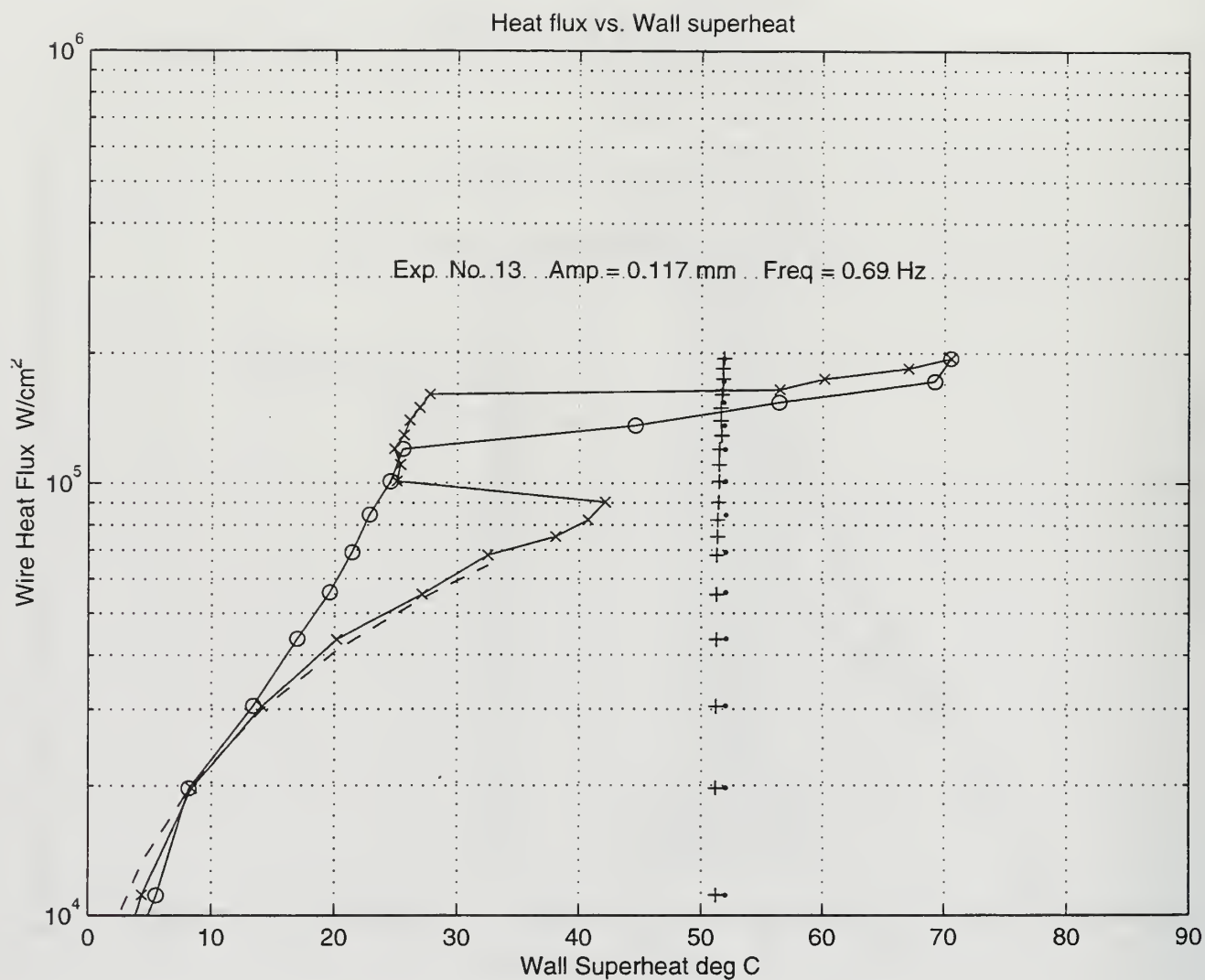


Figure 21. Boiling Curve of FC-72 with an Oscillation of Amplitude 0.117mm and a Frequency of 1.2Hz.

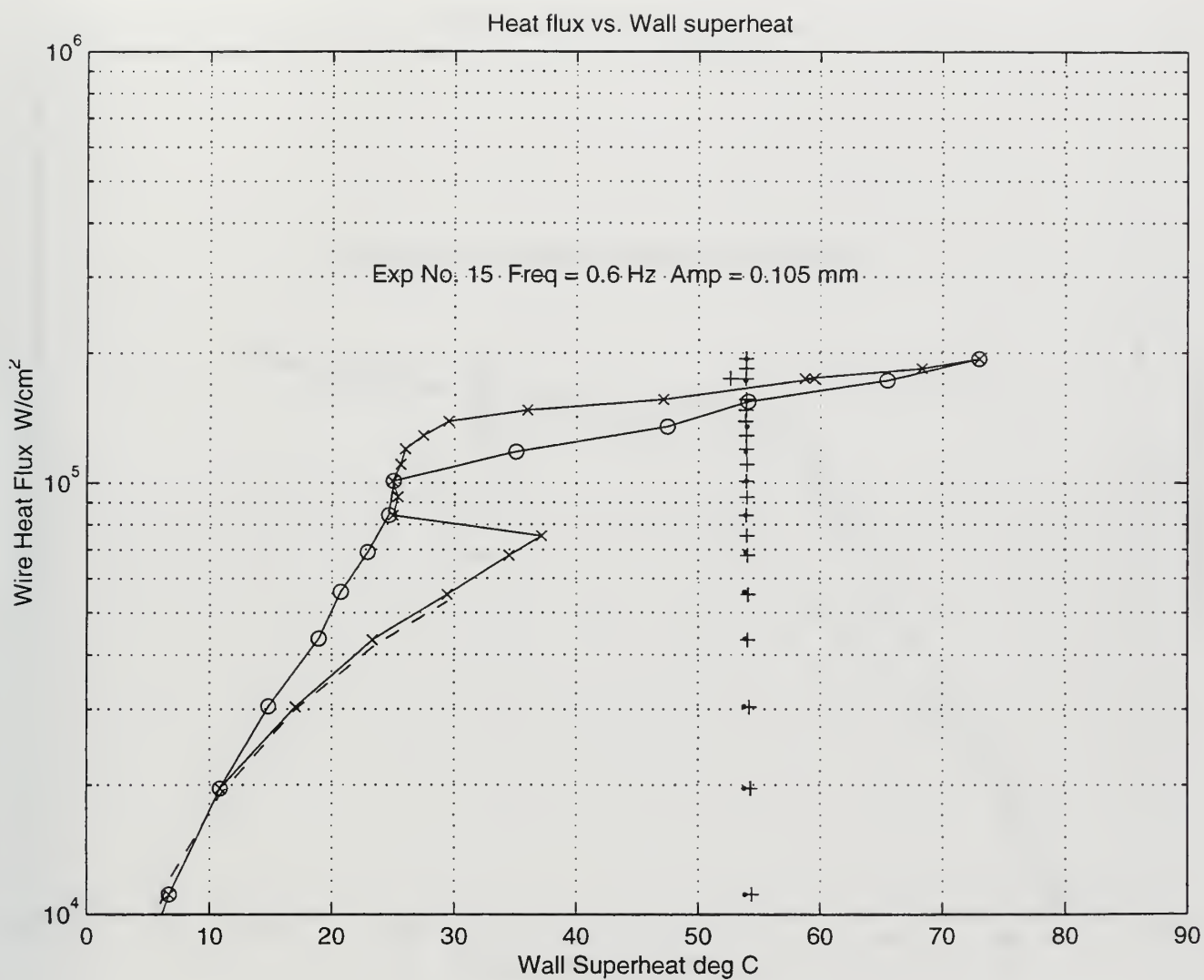


Figure 22. Boiling Curve of FC-72 with an Oscillation of Amplitude 0.105mm and a Frequency of 0.6Hz.

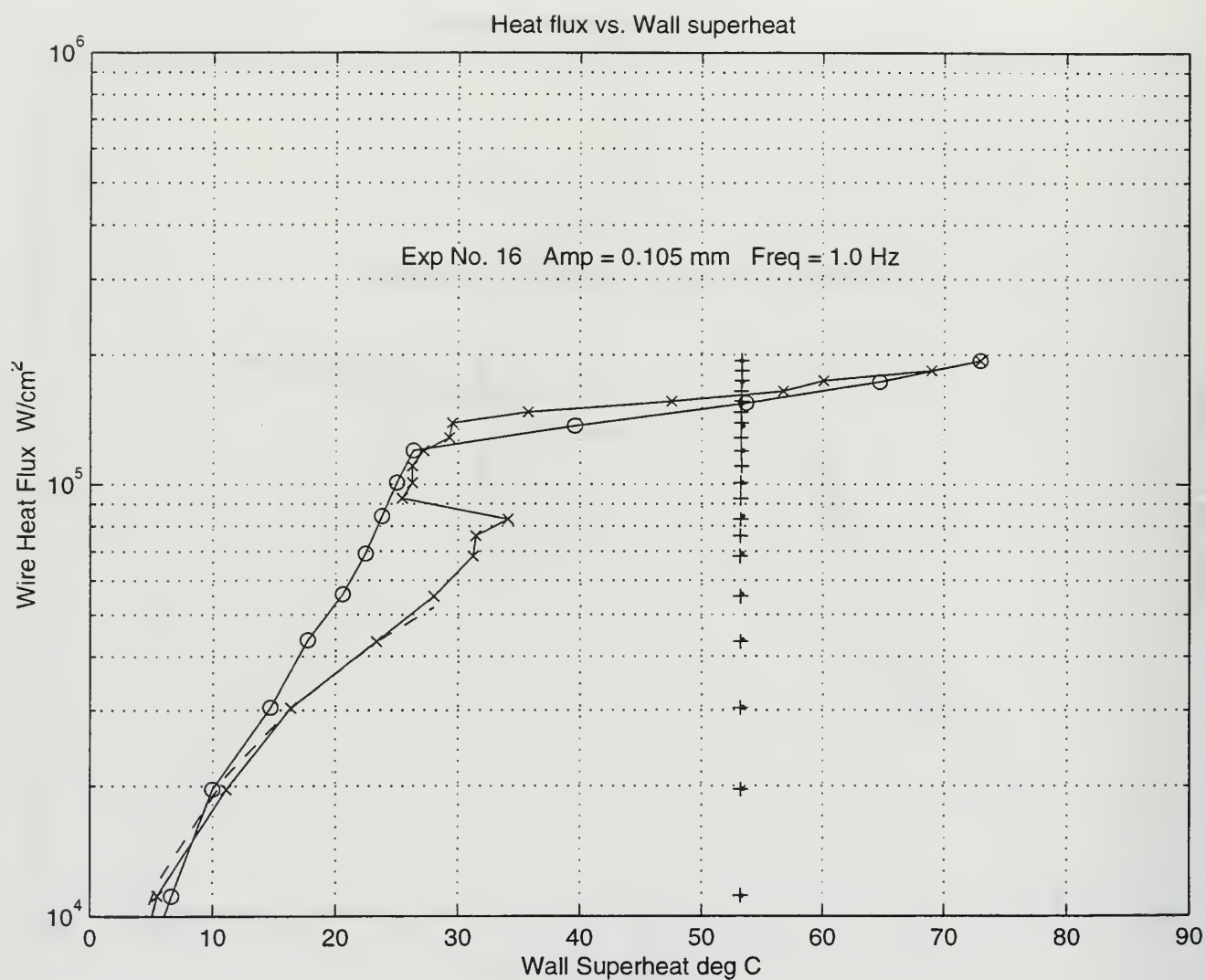


Figure 23. Boiling Curve of FC-72 with an Oscillation of Amplitude 0.105mm and a Frequency of 1.0Hz.

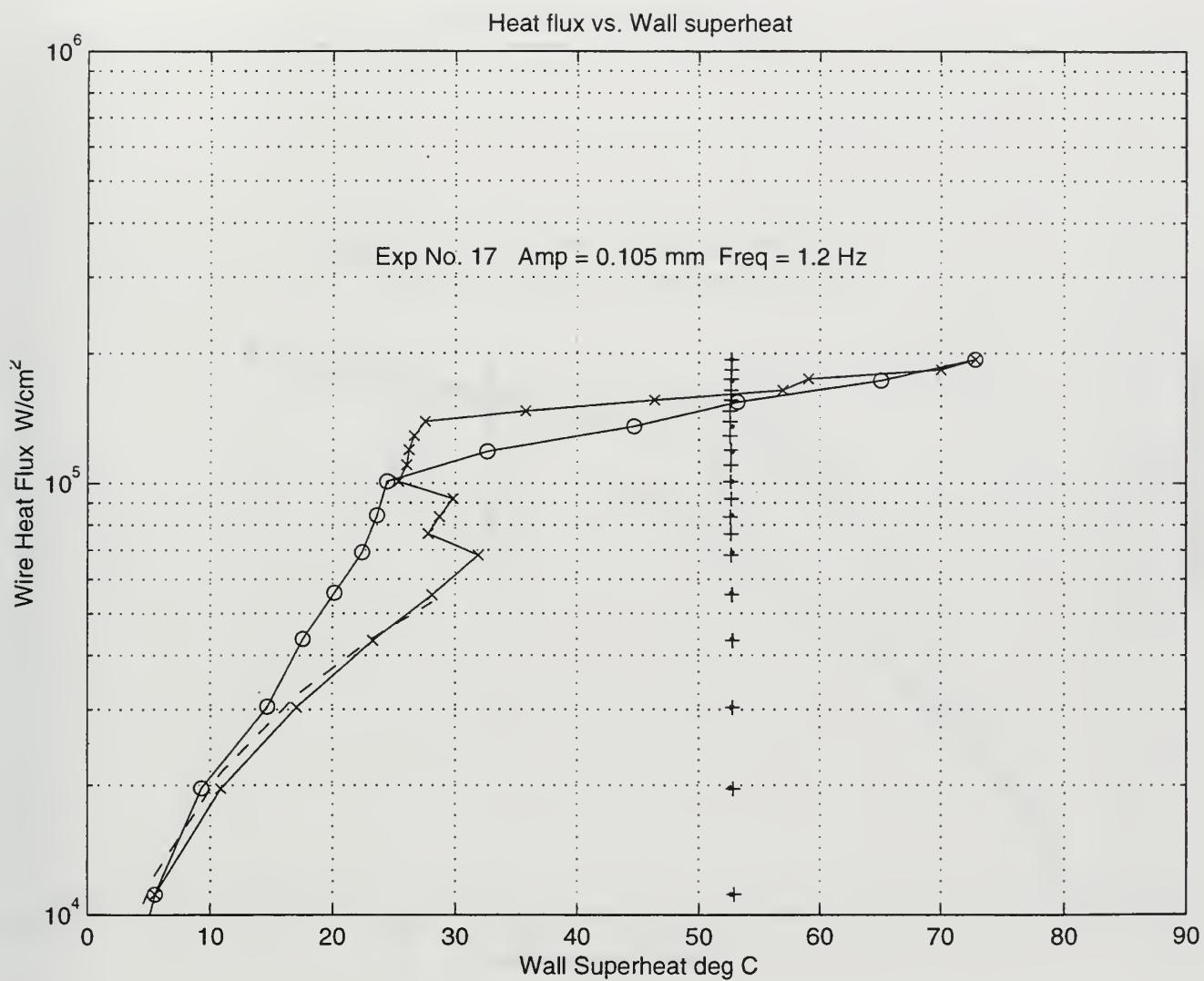


Figure 24. Boiling Curve of FC-72 with an Oscillation of Amplitude 0.105mm and a Frequency of 1.2Hz.

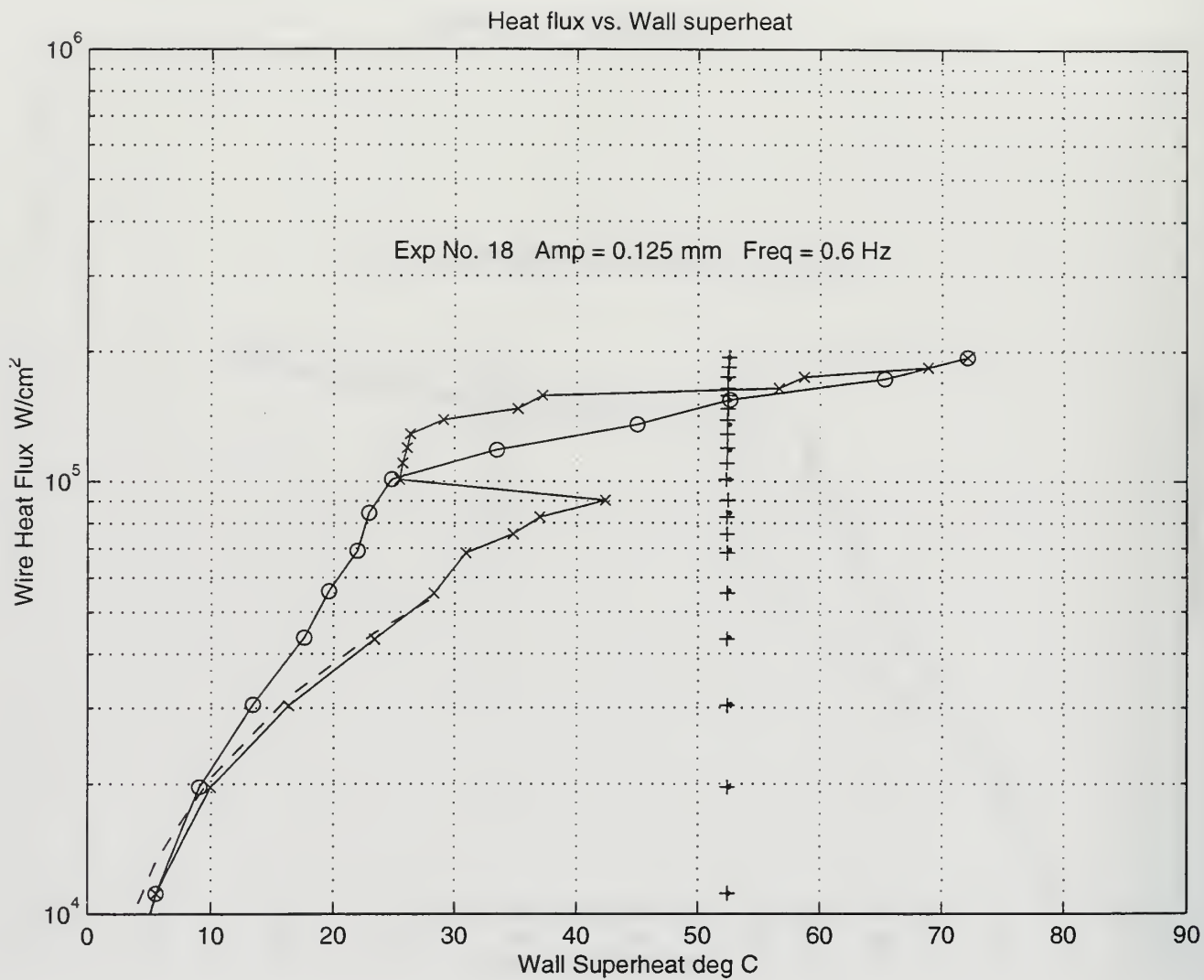


Figure 25. Boiling Curve of FC-72 with an Oscillation of Amplitude 0.125mm and a Frequency of 0.6Hz.

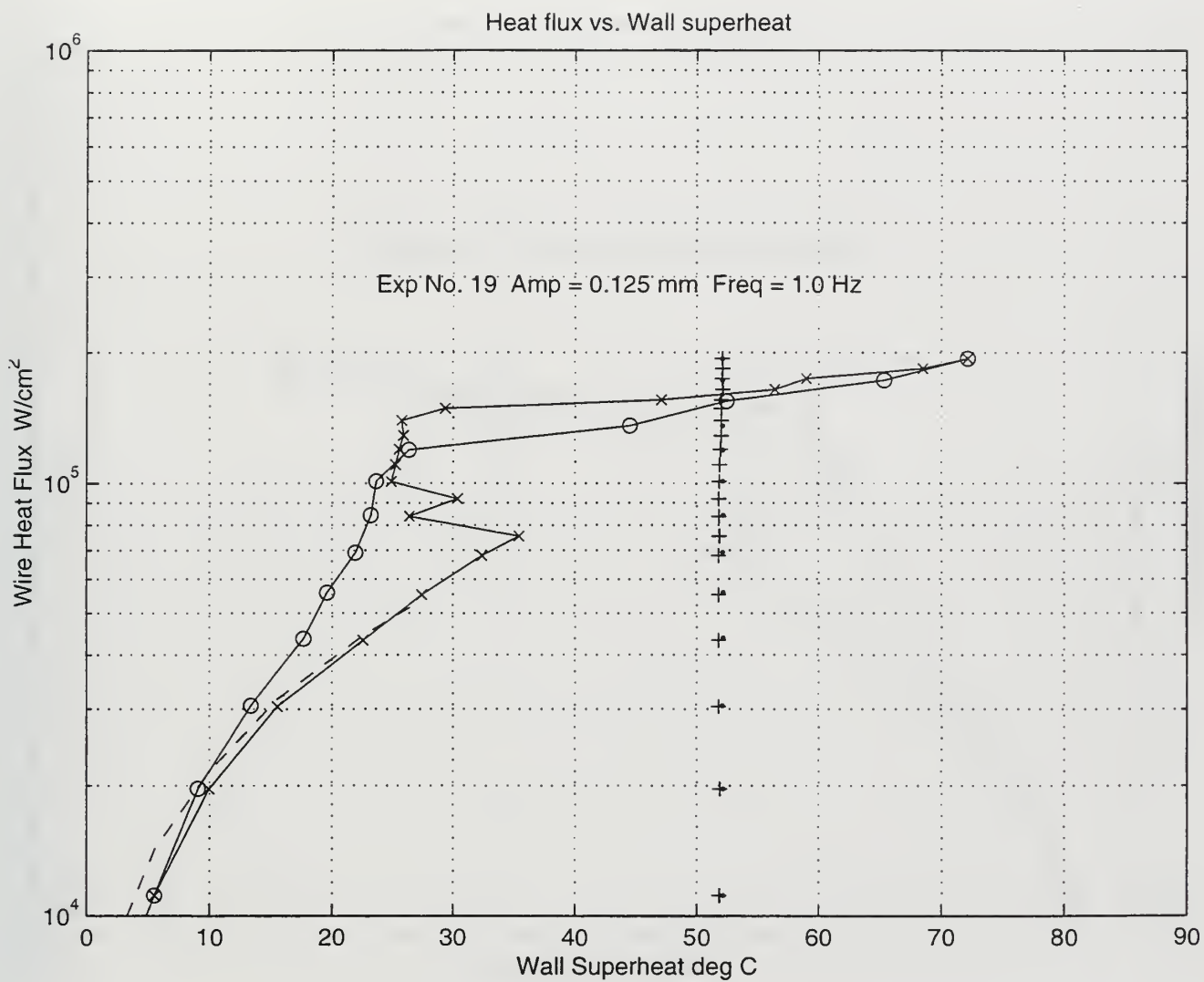


Figure 26. Boiling Curve of FC-72 with an Oscillation of Amplitude 0.125mm and a Frequency of 1.0Hz.

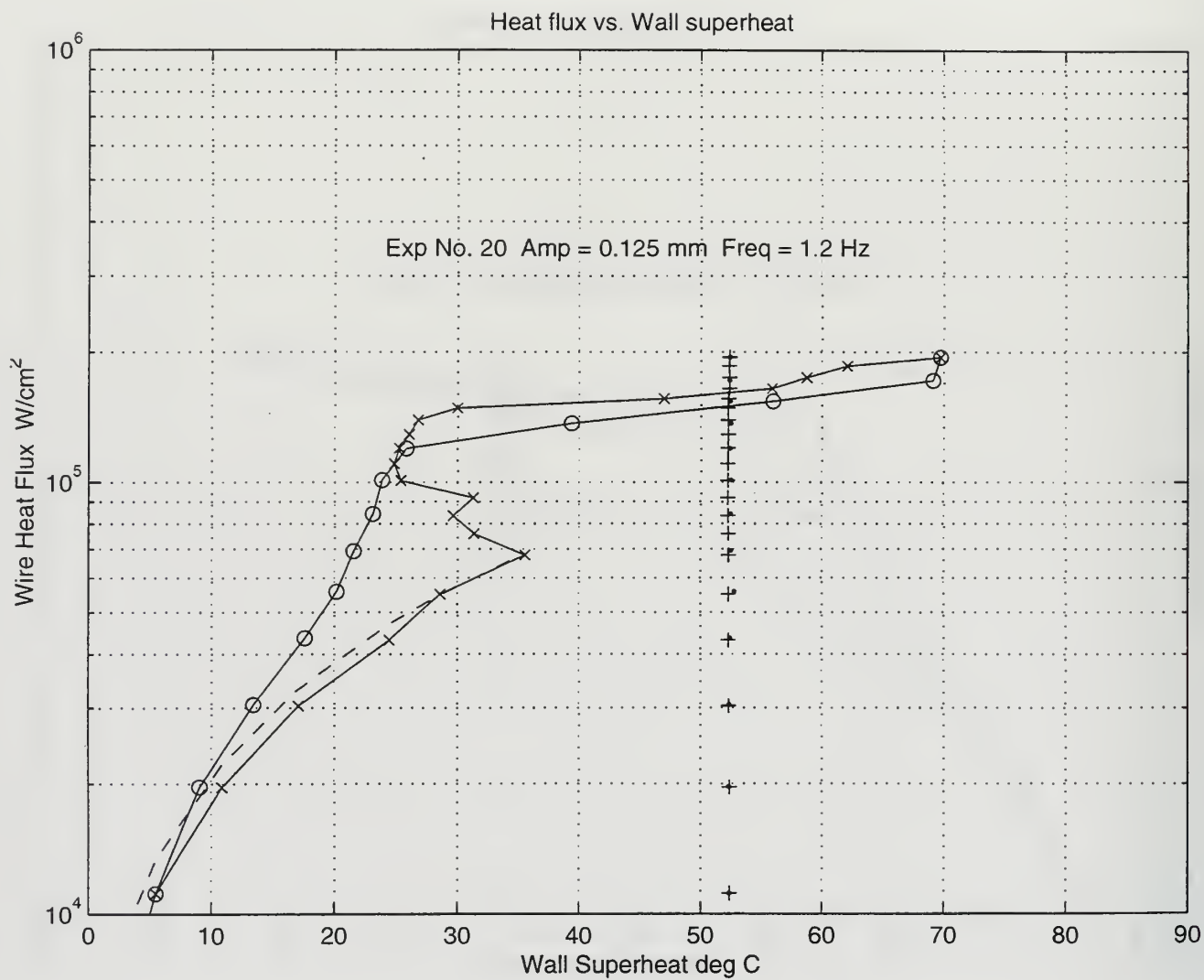


Figure 27. Boiling Curve of FC-72 with an Oscillation of Amplitude 0.125mm and a Frequency of 1.2Hz.

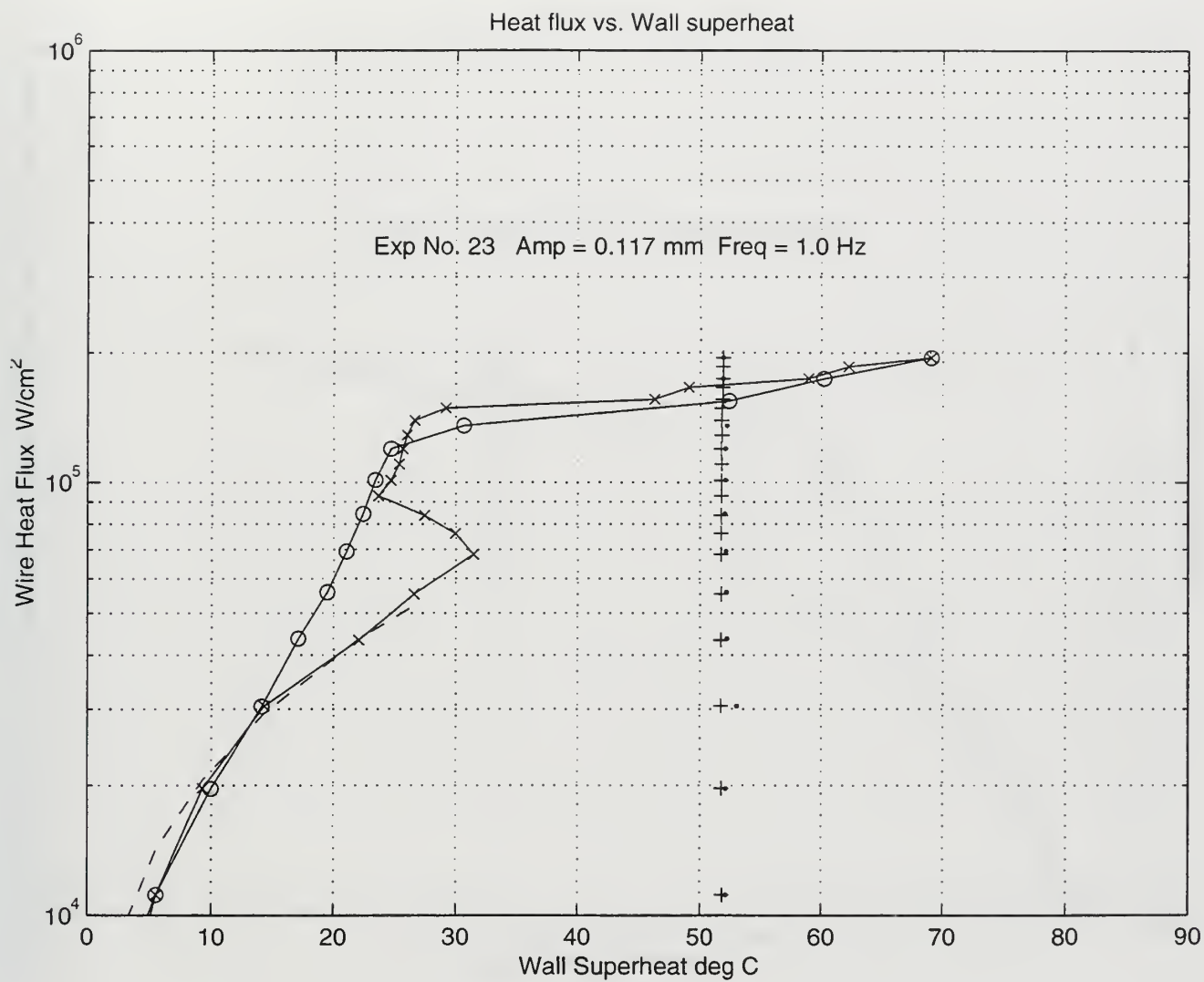


Figure 28. Boiling Curve of FC-72 with an Oscillation of Amplitude 0.117mm and a Frequency of 1.0Hz.

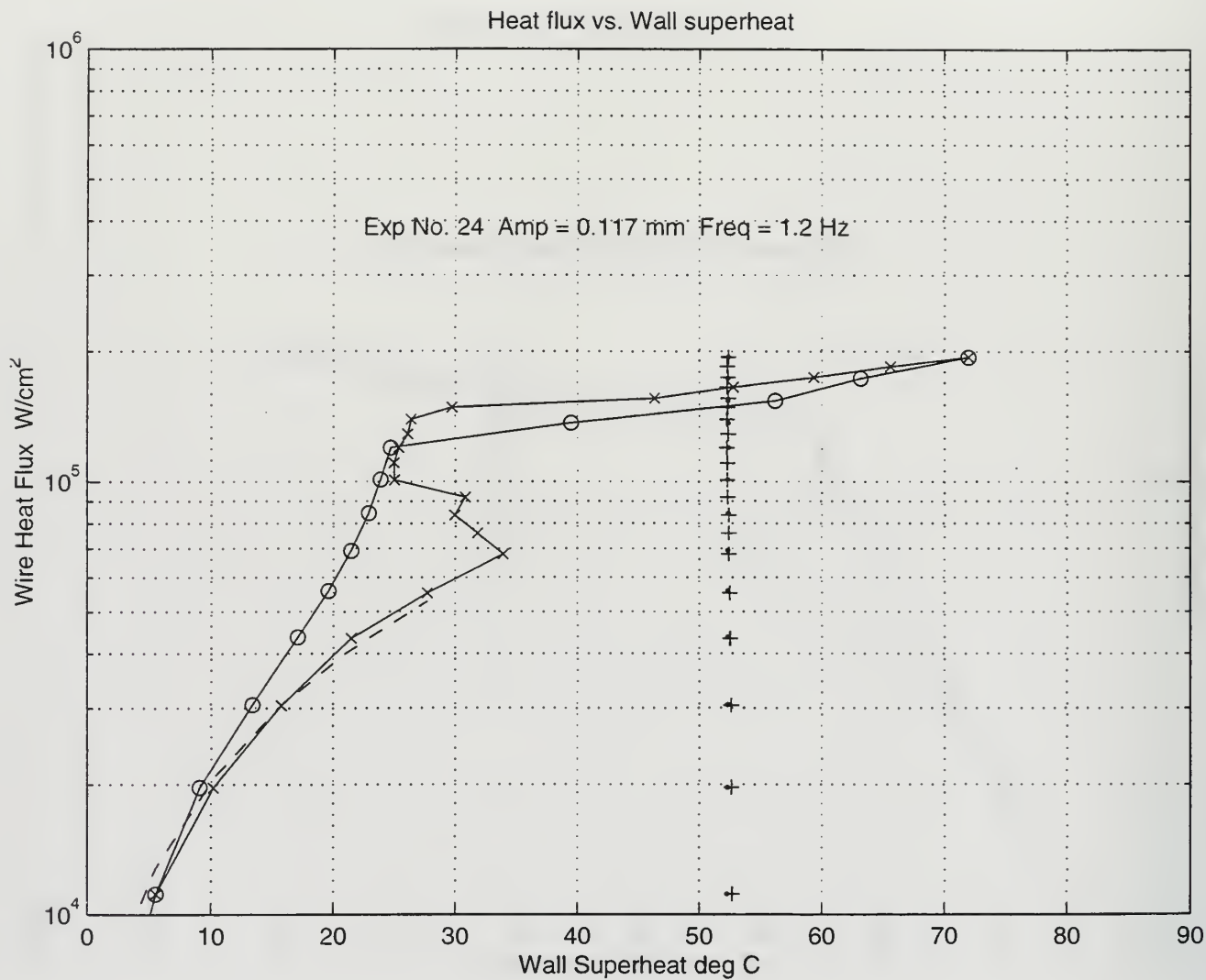


Figure 29. Boiling Curve of FC-72 with an Oscillation of Amplitude 0.117mm and a Frequency of 1.2Hz.

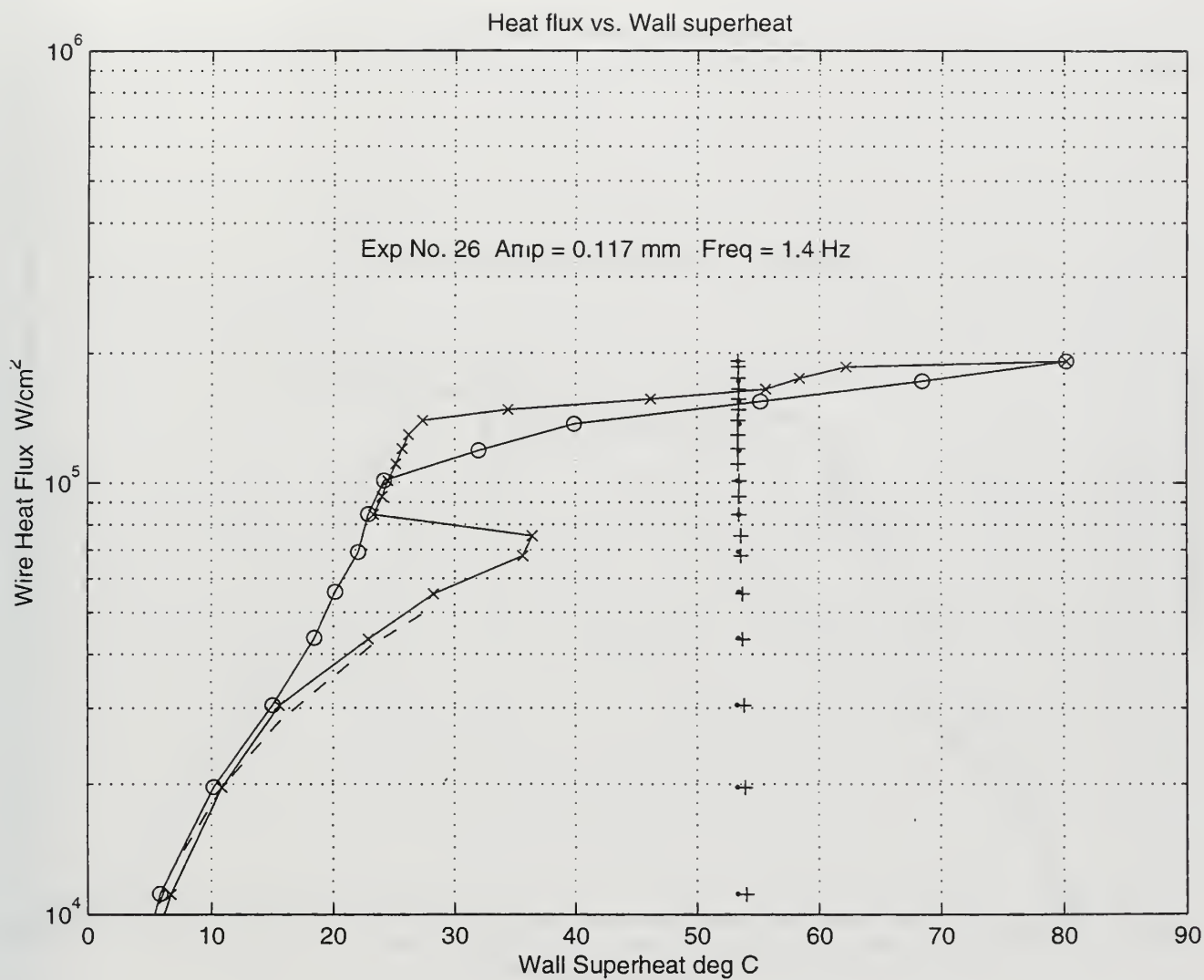


Figure 30. Boiling Curve of FC-72 with an Oscillation of Amplitude 0.117mm and a Frequency of 0.117mm.

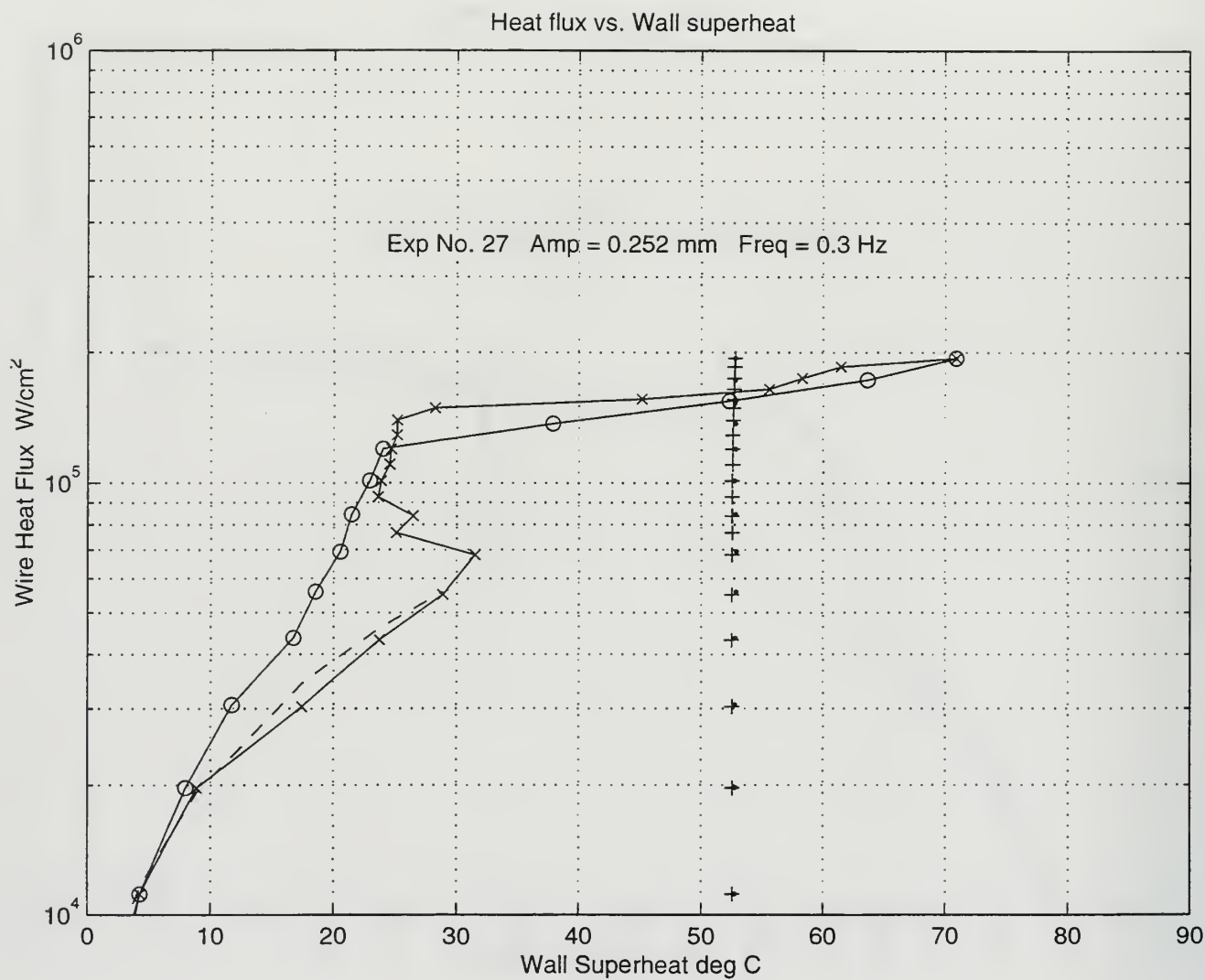


Figure 31. Boiling Curve of FC-72 with an Oscillation of Amplitude 0.252mm and a Frequency of 0.3Hz.

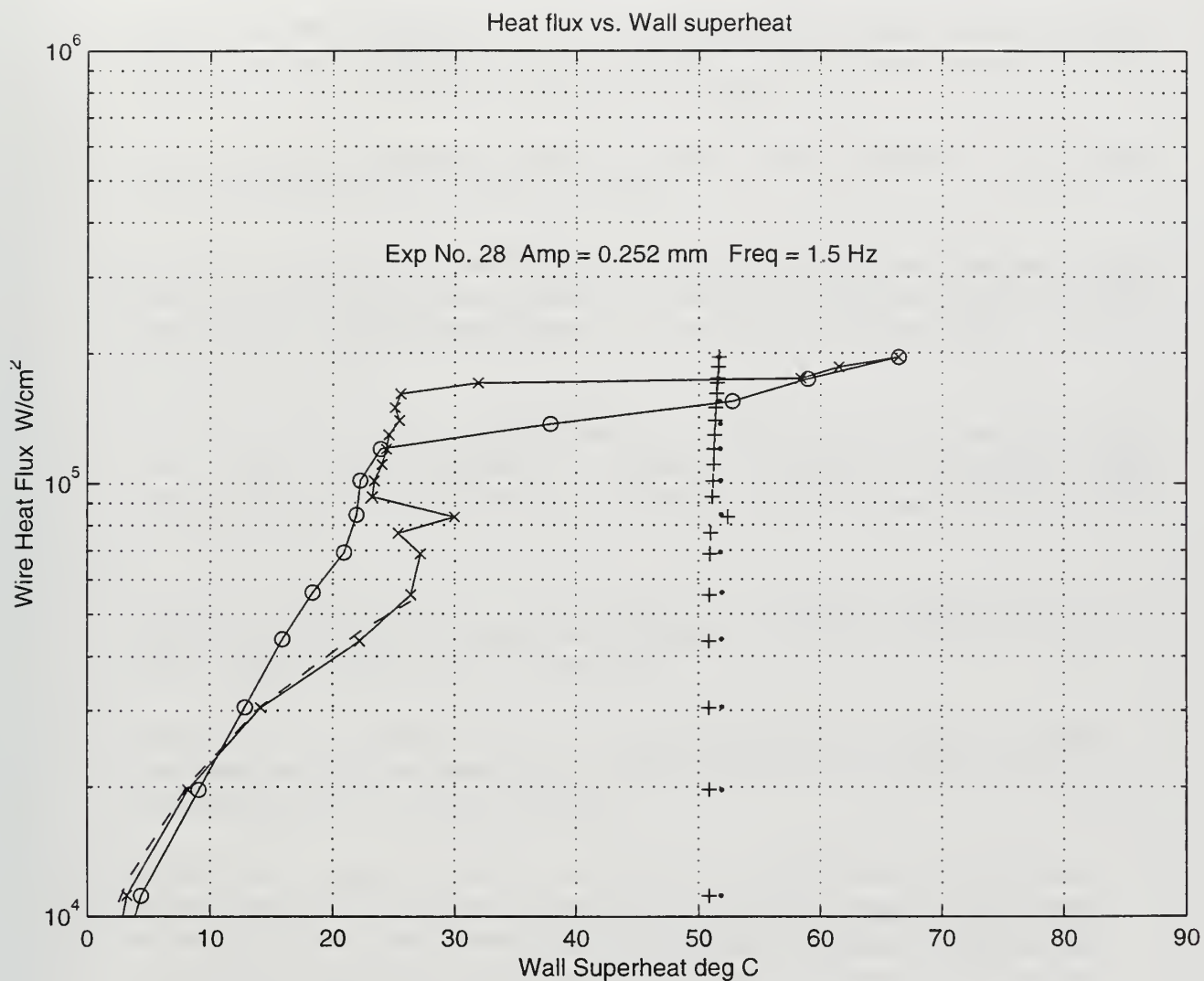


Figure 32. Boiling Curve of FC-72 with an Oscillation of Amplitude 0.252mm and a Frequency of 1.5Hz.

LIST OF REFERENCES

1. Cengel, Yunus A., *Heat Transfer, a Practical Approach*. p.365. WCB McGraw Hill, 1998.
2. Dhir, V.K., *Boiling Heat Transfer*, Annual Review of Fluid Mechanics. 1998.
3. Kuehn, T.H. and Goldstein, R.J., *Correlating Equation for Natural Convection Heat Transfer between Horizontal Circular Cylinders*. International Journal of Heat Transfer, Vol 19, pp.1127-1134, Pergamon Press, 1976.
4. 3M Corporation, *Fluorinert Electronic Liquids Product Manual*, Commercial Chemical Division, St. Paul, Minnesota 1987.
5. You, S.M., Bar-Cohen, A., and Simon, T.W., *Boiling Incipience and Nucleate Boiling Heat Transfer of Highly- Wetting Dielectric Fluids from Electronic Materials*, IEEE Transactions on Components, Hybrids, and Manufacturing Technology, Vol. 13, No.4, December 1990.
6. You, S.M., Simon, T.W., and Bar-Cohen, A., *A Technique for Enhancing Boiling Heat Transfer with Application to Cooling of Electronic Equipment*, IEEE Transactions on Components, Hybrids, and Manufacturing Technology, Vol.15, No. 5, October 1992.
7. You, S.M., Ammernan, G.N., and Hang, Y.S., *Boiling Characteristics of Cylindrical Heaters in Saturated, Gas Saturated, and Pure Subcooled FC-72*, Journal of Heat Transfer, Vol.119, May 1997.
8. Marcellus, M.C., Spilhaus, A.F., Jr., and Troeltzech, L.A., *Heat Transfer Characteristics of Fluorochemical Inert Liquid FC-75*, Journal of Chemical and Engineering Data, Vol. 6, No.3, July 1961.
9. Kelleher, M.D., Egger, R., Joshi, Y., and Lloyd, J.R., *Modification of the Nucleate Boiling Hysteresis in the Pool Boiling of Fluorocarbons*, Heat Transfer 1994, Proceedings of the Tenth International Heat Transfer Conference Brighton UK, Vol.5 pp.87-92, Edited by G.F. Hewitt, Published by Institute of Chemical Engineers, Warwickshire UK. 1994.
10. Turk, Ugur *Boiling of Highly Wetting Liquids in Oscillatory Flow*, Masters Thesis, Naval Postgraduate School, Monterey, California, December 1995.
11. Egger, R.A., *Enhancement of Boiling Heat Transfer in Dielectric Fluids*, Master's Thesis, Naval Postgraduate School, Monterey, California, September 1991.

12. Nukiyama, S., *The Maximum and Minimum Values of Heat Transmitted from Metal to Boiling Water under Atmospheric Pressure*. Journal of Japan Society of Mechanical Engineers, Vol. 36, 1934. (Translation: International Journal of Heat and Mass Transfer, Vol. 9, 1966.

INITIAL DISTRIBUTION LIST

1. Defense Technical Information Center.....2
8725 John J. Kingman Rd. STE 0944
Ft. Belvoir, Virginia 2260-6218
2. Dudley Knox Library.....2
Naval Postgraduate School
411 Dyer Road
Monterey, California 93943-5101
3. Professor M.D. Kelleher.....4
Code ME
Naval Postgraduate School
Monterey, California 93943-5000
4. Naval Engineering Curricular Officer, Code 34.....1
Naval Postgraduate School
Monterey, California 93943-500
5. LT Joseph Tuite.....4
30 Madison Avenue
Kearny, New Jersey 07032

69 290NPG 2930
TH
6/02 22527-200 NLE



DUDLEY KNOX LIBRARY



3 2768 00410844 9